Universidade de Aveiro Departamento de Química

2013

Sara Ferreira Carvalho

Sistemas Aquosos Bifásicos com Líquidos Iónicos e Polissacarídeos

Aqueous Biphasic Systems Composed of Ionic Liquids and Polysaccharides

Universidade de Aveiro Departamento de Química

2013

Sara Ferreira Carvalho

Sistemas Aquosos Bifásicos com Líquidos Iónicos e Polissacarídeos

Aqueous Biphasic Systems Composed of Ionic Liquids and Polysaccharides

Dissertação apresentada à Universidade de Aveiro para cumprimento dos requisitos necessários à obtenção de grau de Mestre em Biotecnologia, ramo de especialização Biotecnologia Molecular, realizada sob a orientação científica da Doutora Isabel Maria Boal Palheiros, Professora Auxiliar no Departamento de Química da Universidade de Aveiro, e coorientação da Doutora Mara Guadalupe Freire Martins, Investigadora Auxiliar no Departamento de Química, CICECO, da Universidade de Aveiro.

Aos meus pais, que me instruíram na força da fé
e na alegria da confiança ☺

O júri

Presidente

Professor Doutor João Manuel da Costa Araújo Pereira Coutinho
Professor Associado com Agregação do Departamento de Química da Universidade de Aveiro

Professora Doutora Isabel Maria Boal Palheiros
Professora Auxiliar do Departamento de Química da Universidade de Aveiro

Doutora Ana Belén Pereiro Estévez
Estagiária de Pós-doutoramento do Instituto de Tecnologia Química e Biológica, ITQB2, da Universidade Nova de Lisboa

agradecimentos

No final desta etapa considero importante reconhecer o valor de todos quantos me apoiaram, lembrando-os com gratidão:

Um especial obrigado à Mara Freire, Isabel Boal e João Coutinho pela partilha de conhecimento e experiência, mas também pelo desafio e apoio que demonstraram.

Agradeço também a todos os colegas de laboratório, pela ajuda e pelo companheirismo de sempre: Ana Maria, Tatiana, Maria João, Ricardo, Hugo, Matheus, Mafalda e Fábio.

Agradeço ainda a todo o grupo Path e miniPath pela entreajuda e disponibilidade em todos os momentos, em particular à Rita Costa, Marta Batista, Neusa Foios, Mónia Martins, Tânia Sintra, Helena Passos, Filipa Claudio, Sónia Ventura e Hugo Ferrão.

Durante este percurso académico foi fundamental o apoio dos amigos de sempre, aqueles que me ajudaram a enfrentar cada obstáculo e a ultrapassar todas as dificuldades de sorriso no rosto. Um muito obrigado à Luísa Santos, à Beatriz Costa, ao Nuno Hélder Silva, ao João Cunha, ao João Santos, à Carla Gonçalves, à Mónica Fernandes e à Ana Ruela.

Em conclusão, quero agradecer aos meus pais, manos e avós por tudo o que fizeram por mim, por serem a Família perfeita que são e por terem educado assim a pessoa que sou hoje.

Palavras-chave Sistemas Aquosos Bifásicos, Líquidos Iónicos, Polissacarídeos, Técnicas de Separação

Resumo

No âmbito da procura de processos de separação mais biocompatíveis e amigos do ambiente, os sistemas aquosos bifásicos com líquidos iónicos constituem uma abordagem alternativa e vantajosa para a extração e purificação das mais diversas biomoléculas.

Neste trabalho pretendeu-se estudar especificamente a capacidade de polissacarídeos, como uma alternativa mais benigna face aos sais normalmente utilizados, para formar sistemas aquosos bifásicos com líquidos iónicos. Para tal, determinaram-se os diagramas de fase e composições das duas fases em equilíbrio para diversos sistemas ternários formados por líquidos iónicos, água e polissacarídeos a 298 K. O estudo destes novos sistemas, combinando diferentes famílias de líquidos iónicos representados por uma variedade alargada de catiões e aniões, com dextranas e maltodextrinas, permitiu avaliar o efeito das características estruturais dos líquidos iónicos, bem como da massa molecular dos polissacarídeos, na capacidade de formação de sistemas de duas fases aquosas. Por fim, e para suportar a sua aplicação como novas técnicas de extração, alguns destes sistemas foram também avaliados no que respeita à sua capacidade para extrair aminoácidos.

A utilização de polissacarídeos, nomeadamente de dextrano e maltodextrina, enquanto moléculas indutoras de *salting-out* para formar sistemas aquosos bifásicos com líquidos iónicos, constituiu o foco principal deste trabalho. Pela primeira vez foi mostrado que existe uma nova classe de sistemas aquosos bifásicos constituídos por líquidos iónicos e polissacarídeos contribuindo assim para o desenvolvimento de técnicas de separação e purificação de uma forma mais eficiente, sustentável e ecológica. Estes sistemas poderão ainda ser vistos como vias promissoras no melhoramento de processos biotecnológicos que tendem a ser cada vez mais decisivos na indústria.

Keywords Aqueous Biphasic Systems, Ionic Liquids, Polysaccharides, Separation Techniques

Abstract

Aiming at finding more biocompatible and environmentally-benign separation processes, aqueous biphasic systems composed of ionic liquids can be envisaged as an alternative and advantageous approach for the extraction and purification of the most diverse biomolecules.

In this work, the main goal consisted on the study of the ability of polysaccharides, as a benign alternative over inorganic salts typically used, to form aqueous biphasic systems with ionic liquids. To this aim, the phase diagrams and respective compositions of the two phases in equilibrium for ternary systems consisting of several ionic liquids, water, and polysaccharides were determined at 298 K. By the combination of different families of ionic liquids, achieved by a representative variety of cations and anions, with dextrans and maltodextrins, it was possible to infer on the effect of the IL structural characteristics, as well as on the polysaccharides molecular weight through the formation ability of aqueous two-phase systems. Finally, and to ascertain on the potential application of these new systems such as extraction techniques, some of them were also used and evaluated regarding their aptitude to extract amino acids.

The use of polysaccharides, namely dextran and maltodextrin, as salting-out molecules to form aqueous biphasic systems with ionic liquids was the main focus of this work. It was demonstrated here, for the first time, that a new class of aqueous biphasic systems composed of ionic liquids and polysaccharides can be formed while contributing to the development of more efficient and sustainable separation and purification techniques. These systems can be also seen as promising routes in the improvement of biotechnological processes which increasingly tend to be decisive in industry.

List of Contents

List of Figures

List of Tables

List of Symbols

Abs – absorbance (dimensionless);

EE% – percentage extraction efficiencies (%);

K – partition coefficient (dimensionless);

M_w – molecular weight ($g \cdot mol^{-1}$);

wt % – weight percentage (%);

α – top and total weight ratio of the mixture (dimensionless);

λ – wavelength (nm);

sd – standard deviation;

R^2 – correlation coefficient;

$[C_2mim][CF_3SO_3]$ - 1-ethyl-3-methylimidazolium trifluoromethanesulfonate;

$[C_4mim][BF_4]$ - 1-butyl-3-methylimidazolium tetrafluoroborate;

$[C_4mim][CF_3SO_3]$ - 1-butyl-3-methyl-imidazolium trifluoromethanesulfonate;

$[C_4mim][EtSO_4]$ - 1-butyl-3-methylimidazolium ethylsulfate;

$[C_4mim][MeSO_4]$ - 1-butyl-3-methylimidazolium methylsulfate;

$[C_4mim][N(CN)_2]$ - 1-butyl-3-methylimidazolium dicyanamide;

$[C_4mim][SCN]$ - 1-butyl-3-methylimidazolium thiocyanate,

$[P_{4441}][MeSO_4]$ - tributyl(methyl)phosphonium methylsulfate;

$[P_{444(14)}]Cl$ - tributyl(tetradecyl)phosphonium chloride

$[P_{4442}][Et_2PO_4]$ - ethyl(tributyl)phosphonium diethylphosphate;

$[P_{4444}]Br$ - tetrabutylphosphonium bromide;

$[P_{4444}]Cl$ - tetrabutylphosphonium chloride;

$[P_{i(444)1}][Tos]$ - triisobutyl(methyl)phosphonium tosylate;

AA – amino acid;

ABS – aqueous biphasic system;

EPS - Extracellular polysaccharide

FDA – Food and Drug Administration;

IL – ionic liquid;

TL – tie-line;

TLL – tie-line length;

UV – ultraviolet;

VOC – volatile organic compound.

1 General Introduction

1.1 Scope and Objectives

This work is focused on the exploitation of feasible polysaccharides capable of forming aqueous biphasic systems (ABS) when combined with ionic liquids (ILs). IL-polysaccharide-based ABS were studied with the aim of finding more benign and sustainable liquid-liquid extraction techniques while envisaging their possible application in the separation of biomolecules or added-value compounds from fermentation broths, industrial wastes or other different media.

This work addresses, for the first time, the evaluation and characterization of different ABS composed of IL + polysaccharide + H_2O. Two families of ILs, phosphonium- and imidazolium-based, and two polysaccharides of different chemical structure and molecular weight, dextran and maltodextrin, were investigated. This selection of phase-forming components allows the inspection on the impact of the IL chemical structure and the polymer nature and molecular weight through the ABS formation ability. The results obtained are divided into three main chapters according to the type of ABS phase diagrams: (i) phosphonium-based ILs + dextrans; (ii) phosphonium-based ILs + maltodextrins; (iii) imidazolium-based ILs + maltodextrins. For each system, the ternary phase diagrams were determined by means of their solubility curves, tie-lines (TLs) and tie-line lengths (TLLs) at 298 K. Finally, a selection of the characterized systems was tested in what concerns their extractive potential for different amino acids (L-tyrosine, L-tryptophan and L-phenylalanine) as a demonstrative example.

The results gathered in this work are expected to enlarge the plethora of IL-based ABS towards the finding of greener, sustainable and more environmentally-friendly systems.

1.2 Aqueous Biphasic Systems (ABS)

As stated by the United Nations[1], biotechnology is defined as any technological application that uses biological systems, living organisms, or derivatives thereof, in order to solve problems or create useful products. Indeed, biotechnology provides tools for developing processes that are eco-efficient and

products that are not only more profitable but also more environment-friendly, and is already considered a great alternative to the conventional chemical processes[2]. In fact, the large scale production of compounds with complex structures and high value-added using biotechnological processes has increased mainly because these allow less wasteful use of materials and energy, enable a greater and more efficient use of renewable resources, and improve the production of compounds which are less toxic, easily recyclable, and biodegradable[3].

In general, a biotechnological process can be divided into three steps: feed-stock preparation; bioconversion; and product recovery. This latter step is often faced with complicated techniques involving several stages, the use of organic and volatile solvents, and high energy demands to achieve the desired separation or purification level[4]. Advances in biotechnology represent a great potential for application in a wide range of industrial fields, but there is a clear need for cost-efficient, scalable and feasible process for bioseparation. It is essential to develop new approaches for the purification of biomolecules from complex media, such as fermentation broths. Moreover, for most biomolecules of interest (proteins, enzymes, nucleic acids, cell organelles, antibiotics…) it is crucial to preserve their biological activity by maintaining the pH, temperature or osmotic pressure conditions throughout the process of purification.

Currently, the liquid-liquid processes that are used to extract biocompounds from liquid solutions may be cast into two main types: liquid-liquid extraction using water-immiscible-organic-solvents and aqueous biphasic systems (ABS). This last approach, where the partitioning occurs between two aqueous liquid phases, is preferentially used in the purification of biomolecules due to its high effectiveness, high yield, improved purity degree, proper selectivity, technological simplicity, low cost, and avoidance of volatile organic solvents use[5].

ABS were firstly reported by Albertsson[6] who clearly presented their advantages; in fact, fast mass transfer and equilibrium are achieved, requiring little energy, and so, ABS are cost-effective processes. Moreover, reliable scale-up and use in continuous operation processes are possible, which make those systems attractive for industrial applications[7].

ABS are ternary systems mainly composed of water and two solute combinations; the two phase system is formed by mixing two incompatible compounds, yet both water-miscible, in which, above a critical concentration, the spontaneous phase separation takes place. Conventional ABS are commonly formed by polymer-polymer, polymer-salt or salt-salt combinations[8]. After mixing, the phase separation occurs, as it is shown in the example of Figure 1, and the biomolecules tend to partition among the two phases. The phases' separation is usually achieved by gravity sedimentation or centrifugation. By the adequate choice of the ABS components, it is possible to obtain the biomolecule in one phase and the related contaminants in the other phase, hence leading to the purification of the target species. As both phases have a great amount of water in their composition, these systems are able to preserve the native conformation and the biological activity of biomolecules in solution which embodies a major advantage[9].

Figure 1. Macroscopic appearance of an IL-based ABS.

Due to the described associated features, ABS have been studied and applied in the separation of biomolecules from diverse and complex media, for instance, from fermentation broths, wastewater effluents, biological suspensions, commercial sources, among others[10]. Therefore, the interest in ABS has been increasing, leading to numerous studies and publications focused on this topic. Figure 2 shows the upward trend of manuscripts published in the last 10 years regarding ABS.

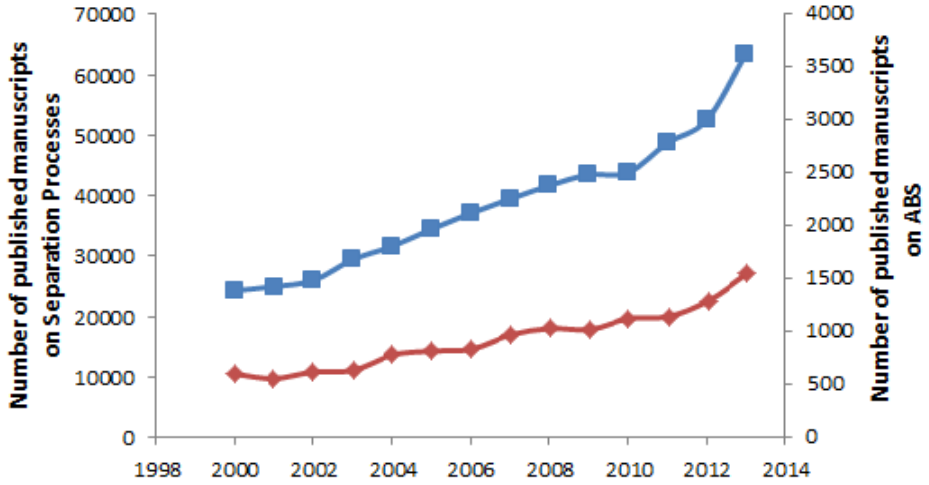

Figure 2. Number of published manuscripts *per* year concerning separation processes: in general (■) and ABS (◆). Consulted on ScienceDirect.com on 30th October of 2013.

Before implementing their use in separation procedures, ABS must be fully characterized, namely each phase diagram (the binodal curve and the respective tie-lines (TLs)) that describes the system behavior for a given pH or temperature conditions must be obtained. The binodal curve represents the separation between the monophasic and the biphasic regions; all mixtures with compositions below the binodal curve remain in a homogeneous mixture, while those above this line form two immiscible aqueous phases (liquid-liquid demixing). Phase diagrams are commonly described by orthogonal representations where the concentration of water is omitted. The vertical axis is used for the solute that is enriched in the top (less dense) phase and the horizontal axis is used for the representation of the second compound concentrations, as shown in Figure 3.

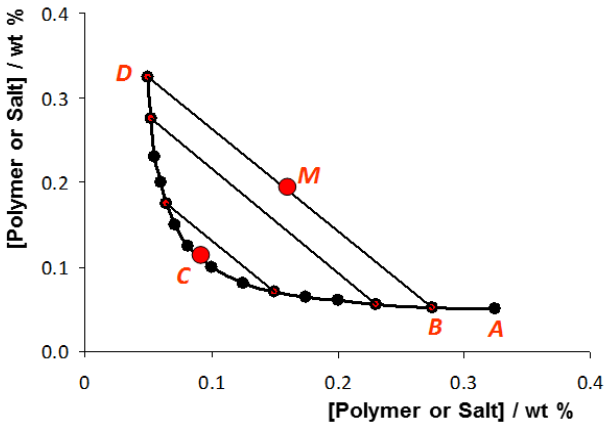

Figure 3. Orthogonal representation of a phase diagram. Adapted from Freire et al.[8]

In this example, *M* represents a total mixture composition that falls into the biphasic region; the binodal curve is presented by the black curve passing through *DCBA*; the compositions of each phase are depicted by the points *D* and *B*, the end-points of the TL represented by the parallel lines[8]. Tie-line length (TLL) is another parameter commonly used to describe these systems and is a numerical indicator of the composition difference between the two phases, which is usually used to correlate trends in the partitioning of solutes among the coexisting phases[8]. Beyond that, it should be remarked that the separation performance is largely affected by important characteristics of the phases, such as chemical composition, density and viscosity[11].

1.3 Novel ABS Composed of Ionic Liquids and Polysaccharides

Nowadays, many researchers are joining efforts to find new ways and new compounds that can be used to form ABS and to improve the separation yields toward more sustainable approaches. Besides the conventional polymer-based ABS, a new sort of aqueous systems has emerged in the last decade. Rogers and co-workers[12] reported, for the first time, that ionic liquids (ILs) can be also used to form ABS when mixed with concentrated inorganic salt aqueous solutions (particularly K_3PO_4). Since then, a large number of publications have appeared in literature regarding ABS constituted by ILs and several molecular species (*e.g.* salts, amino acids, carbohydrates and polymers).[8] Figure 4 depicts the trend of publications regarding IL-based ABS, either with different ILs or different salting-out species[8].

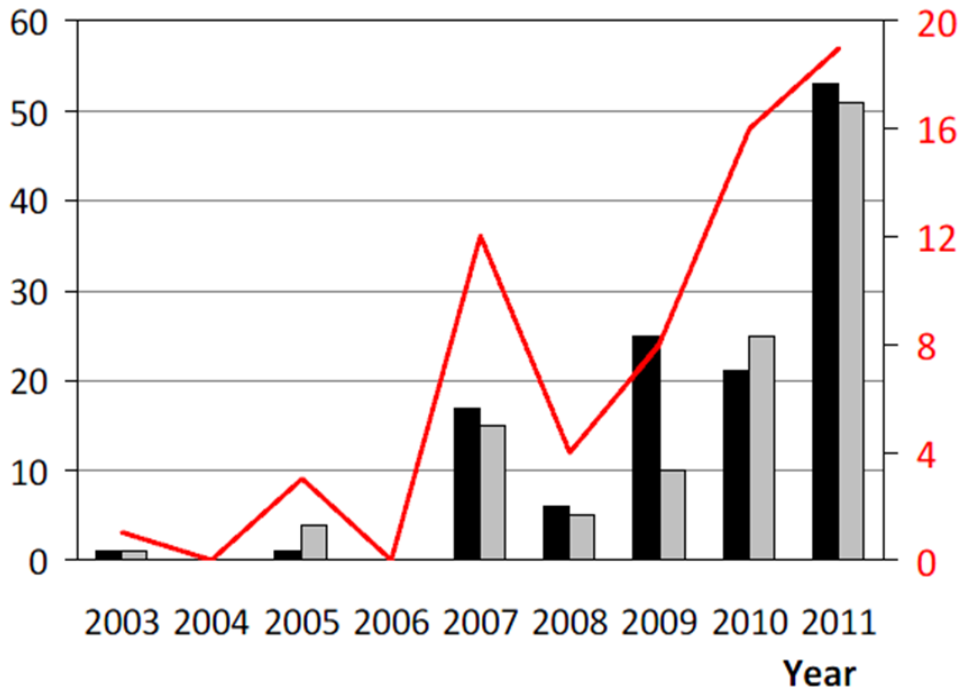

Figure 4. Phase diagram data for IL-based ABS from 2003 to 2011: number of articles *per* year (red line/scale); number of distinct ionic liquids studied *per* year (black bars); and number of distinct salting-out species evaluated *per* year (grey bars)[8].

1.3.1 Ionic Liquids

The increasing interest on the use of ILs mainly arose from their outstanding capability to perform as improved solvents. Several physical and chemical properties have been described and that confer to them additional advantages over conventional organic solvents, namely negligible vapor pressures (do not evaporate at atmospheric conditions) and thermal stability up to high temperatures[13, 14, 15, 16]. Thus, ILs combine conventional salt properties (since they are composed of ions) with those of organic solvents (they are liquid at temperatures below 373 K and are able to dissolve a wide variety of solutes)[17-19]. Due to their unique and attractive physicochemical properties, ILs have been applied in catalysis[19, 20], organic synthesis[21], chemical or enzymatic reactions[22, 23], multiphase bioprocess operations[24], mass spectrometry analysis[25] and in biofuel production[26].

ILs can be grouped into different families according to the cation core. Pyrrolidium-, imidazolium-, piperidium-, pyridinium-, ammonium- and

phosphonium-based are some of the common IL families. Their cation chemical structures are presented in Figure 5.

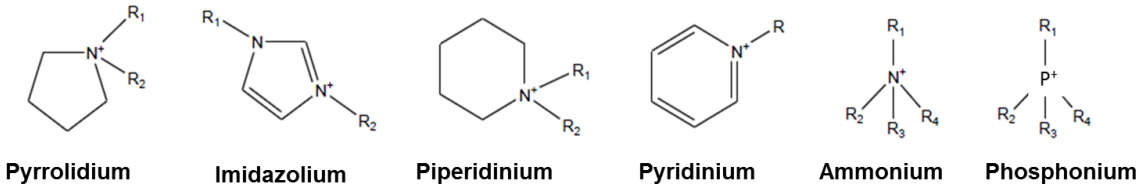

Figure 5. Exemplar IL cation structures.

On the other hand, the anions which compose an IL can range from simple halogenates to more complex anions, such as acetate, tosylate, dicyanimide, thiocyanate, sulfate, triflate, among others ions. Exemplar ILs anion structures are presented in Figure 6.

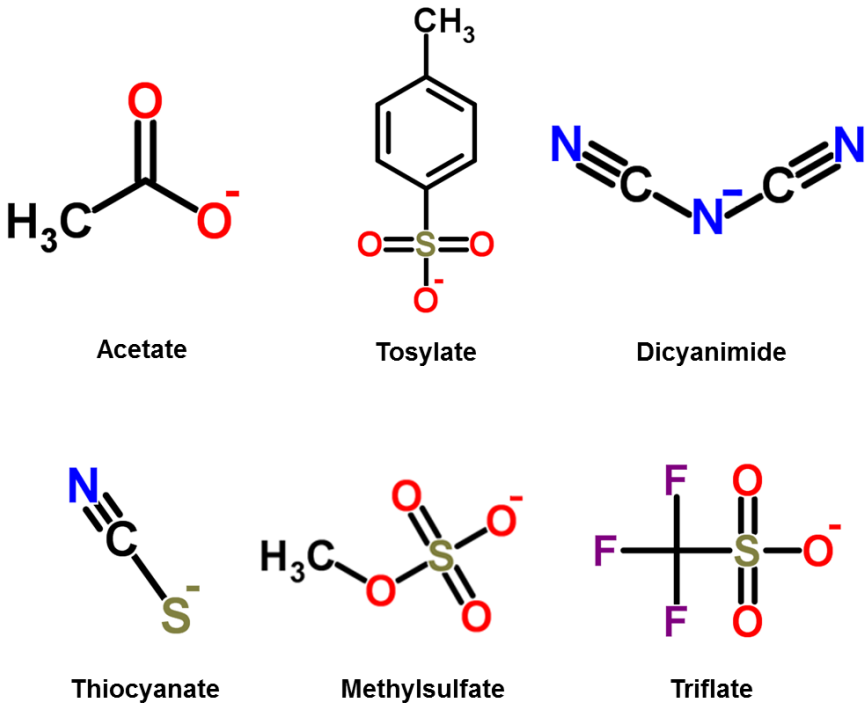

Figure 6. Exemplar IL anion structures.

Imidazolium-based ILs constitute one of the most widely studied families, and in which the positive charge of the *N*-alkyl-substituted imidazolium cation is balanced with an inorganic/organic anion. Based on the cation cores, the non-aromatic ILs, such as pyrrolidinium, piperidinium and phosphonium[27] seem, *a priori*, to be more benign than the aromatic-based compounds (imidazolium and

pyridinium). Yet, phosphonium-based ILs have been a poorly studied family, which may result from the relative abundance of commercially available amines compared with the small variety of phosphines[27].

Several studies on IL-based ABS have reported outstanding results on separation, concentration and purification of proteins[28-29], heavy metal ions[30-31], small organic molecules[32], and antibiotics[33]. IL-based ABS display enhanced advantages over the more conventional polymer-based systems, such as little emulsion formation, low viscosity, quick phase separation and high extraction efficiency which can be easily manipulated by a proper selection of the ions composing a given IL[34]. Due to the vast diversity of cation/anion combinations, IL-based ABS cover a wider hydrophilic-hydrophobic balance at their coexisting phases when compared to conventional systems composed of polymers[35]. This tailoring ability is highly advantageous for the separation of different kinds of solutes using ABS[36].

1.3.2 Polysaccharides

Despite the innovations on ABS described above and the interest dedicated to IL-based ABS formed by the addition of inorganic salts[12, 17, 37], further improvements on their sustainable and biocompatible character are still required. In fact, commonly used salts, such as K_3PO_4, release high amount of phosphate ions into the aqueous media, and thus complicate the ILs recycling process as they also dissociate in aqueous solution. In addition, the presence of these ions may lead to highly alkaline and/or high ionic strength solutions which can be harmful for some biomolecules[38]. Although the most studied systems are still composed of ILs and salts, other species have been considered to replace those highly charged systems, namely amino acids[39-40], carbohydrates[38,41] and polymers[42].

The use of carbohydrates to replace salts in IL-based ABS can be highly advantageous due to their biodegradable, non-toxic and non-charged nature. Previous studies showed that carbohydrates (mono- and disaccharides) have high

affinity to water and are capable of undergoing liquid-liquid demixing in the presence of an IL aqueous medium, giving rise to ABS[38,43].

The focus in carbohydrates has emerged in several fields and applications; particular attention has been paid to microbial polysaccharides due to their innovative applications as gelling, emulsifying and stabilizing agents, which are important in many different technologies, such as in the food, clinical or agricultural areas[44, 45]. Extracellular polysaccharides, or exopolysaccharides (EPS)[46], are carbohydrate polymers, typically of high molecular weight and variable composition, that possess a wide variety of chemical and physical properties, enabling extensive applications in food, pharmaceutical, oils, cosmetics, textiles, inks and agricultural products, among other industries[47, 48]. These compounds may have a wide variety of sources, such as algae (alginate, agar, carrageenan), seeds (gums), tree exudates (gum arabic and karaya), microbial biosynthesis (xanthan, gellan, dextran, curdlan), and others produced by chemical modifications of natural polysaccharides (pectin, gelatin, starch)[47-49]. Nowadays, microbial polysaccharides are amongst the most studied carbohydrates due to their advantages, namely a production independent of weather conditions, regional raw materials and rapid processes. Indeed, microbial polysaccharides can be produced under controlled conditions and with selected species[47]. Dextran and maltodextrin constitute two well-known examples of natural polysaccharides that are currently the targets of intense research. The chemical structures of the two polysaccharides are presented in Figure 7.

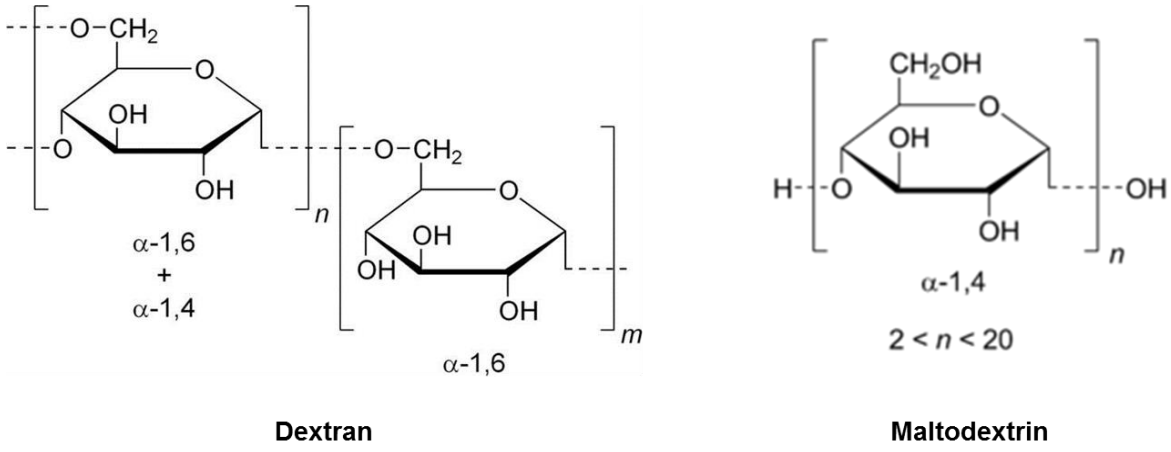

Figure 7. Chemical structure of polysaccharides: dextran and maltodextrin.

Dextran is a homo-polymer of glucose, which means that it is a high molecular weight molecule (≥ 1000 Da) composed of α-D-glucose chains predominantly linked by α(1→6) glycosidic linkages. There can be also small D-glucose side chains branches with α(1→2), α(1→3), or α(1→4)-linkages, which confer to this molecule a great diversity in molecular weight and spatial arrangement. The type and the length of branch chains, and consequently their physical and chemical properties, depend on the microbial producing strains and culture conditions[50, 51], but, for the mostly used strain (*Leuconostoc mesenteroides* NRRL B-512(F)), the branching degree is generally less than 5 %[52]. Its properties are viewed as favorable and very versatile, since this long-chain and high-molecular-weight molecule disperses in water and gives rise to improved rheological (gelling, thickening) or physical and chemical properties (emulsion stabilization, particle suspension,…) – important tools for the formulation of several products[50, 53]. Dextran has important clinical applications in the production of fine chemicals such as plasma substitutes (blood/plasma volume expanders)[54]. It also finds other industrial applications in food, pharmaceutical and chemical industries as adjuvant, emulsifier, carrier and stabilizer[46, 47, 55, 56]. In food industry it is being used for a wide variety of purposes: in improving textures in milk drinks, yoghurts, jams and ice creams, among other products; in preventing sugar crystallization; in improving moisture retention; and in maintaining products' flavors and appearance[55]. Dextran applications also extend to varied fields as cosmetic products, photography industry, wastewater treatment and laboratory uses[56]. Furthermore, dextran is mostly used in the separation and purification of biological active substances (*e.g*. Sephadex, a cross-linked dextran)[54].

Due to its numerous industrial applications dextran is actually largely produced. In Europe, commercial dextran is mainly produced by *Leuconostoc mesenteroides*, which are GRAS (Generally Recognized As Safe)[57] micro-organisms, known as non-pathogenic, maintaining a safe history in their use in the European Union[53].

As can be seen in Figure 7, dextran presents several -OH groups in its structure. Dextran displays a high water solubility and the solution's viscosity depends on its concentration, temperature, and molecular weight[50]. Due to its

affinity towards water, dextran is a likely candidate to ABS forming. In fact, this polymer is commonly used on polymer-polymer ABS formulations[58]. However, despite its potential to be used as a two-phase inducer, no studies using dextran forming IL-based ABS were found in the literature.

Also with interesting properties and potential, maltodextrin (Figure 7) is a purified concentrated mixture of sugar polymers linked primarily by α-(1→4) D-glucose chains with variable length, and α-(1→6) bonds[59, 60]. Maltodextrins can be considered as low molecular weight analogues of dextran as they are also composed of a glucose-linked backbone with short branches (the backbone is linked by 1−4 bonds, branches are linked to the backbone by 1−6 bonds). Commercial maltodextrins are prepared by partial hydrolysis of starch and are usually described as a white, hygroscopic powder or granules, freely soluble or dispersible in water[61]. Figure 7 shows the maltodextrins common chemical structure, which usually have a dextrose equivalent (DE) value < 20. DE describes the average degree of conversion of starch to dextrose and is known to be inversely proportional to the average molecular weight[62, 63]. As dextran, maltodextrin is rich in –OH groups and highly soluble in water, and thus, can be studied as a phase-forming component of ABS constituted by ILs.

The combined use of carbohydrates and ILs to induce ABS can be regarded as a step towards profitable processes envisaging cleaner and cost-effective approaches. Several works already exist in literature, with phase diagrams reported for ABS composed of several ILs, and monosaccharides (*e.g.* glucose and xylose)[38, 41, 64, 65], disaccharides (*e.g.* sucrose and maltose),[38, 43, 65-67] or polyols (such as sorbitol, xylitol, and maltitol)[38]. These studies[38, 41, 43, 64-67] were devoted only to carbohydrates of low molecular weight and that behave as weak salting-out agents. Therefore, few IL-based ABS have been characterized since they are limited to a restricted number of ILs that are able to create a two-phase system[8]. In this context, there is still the need of finding proper and alternative ILs able to form ABS with carbohydrates and to move to higher molecular weight saccharides, namely polysaccharides. However, no literature data regarding the formation of ABS composed of polysaccharides and ILs were found hitherto.

2 Phosphonium-based ILs + H_2O + dextran

2.1 Introduction

Aqueous biphasic systems have found widespread use in separation and purification approaches. Since greener and more environmentally-friendly concepts are required when considering the use of any new process at the industrial level, ABS have been intensively studied and improved due to their less aggressive character achieved by the high water content at their coexisting phases. Furthermore, given the outstanding properties of ILs, IL-based ABS display high extractive performances[8] gathered by the vast possibility of chemical structures which allow their tailoring.

In the continuous search for more benign ABS, some researchers turned to ternary phase systems composed of ionic liquids + carbohydrates + water[38, 39, 41, 43, 64-67]. The use of carbohydrates to induce IL-based ABS can be seen as a forward step towards greener processes, since they are non-toxic and renewable resources[8]. Still, it should be noted that carbohydrates are weaker salting-out agents[38], and not very well known in this purpose and thus require further investigation. Despite the use of mono- and disaccharides, as well as polyols, to induce the formation of IL-based ABS[38, 41, 43, 64-67], the use of polysaccharides (expected stronger salting-out agents due to their higher molecular weight) was previously not attempted. On the other hand, all the literature reports only considered imidazolium-based ILs to form ABS with carbohydrates[38, 41, 43, 64-67]. However, and as noticed before, phosphonium-based ILs, a poorly studied IL family, are produced in large scale and are comparatively cheaper than the imidazolium-based counterparts, and therefore open a great window of opportunities[68].

Currently, phosphonium-based ILs, with a tetraalkylphosphonium group, $[R_4P]^+$, are delivered for many industrial and pharmaceutical applications[68]. Recent investigations reported their use as solvents in extraction and chemical synthesis, and in corrosion protection[69, 70]. Phosphonium-based ILs present other advantageous properties comparatively to the corresponding ammonium and imidazolium ones: they are thermally more stable, have an enhanced chemical stability under varied conditions, are compatible with strongly alkaline solutes, do

not contain acidic protons, they are inert in most systems (which is a real advantage considering their recycling), among others[70].

Dextran is a carbohydrate usually present in several culture media; it is neutral, biocompatible, biodegradable and stable for a long period of time[71]. Due to the large number of hydroxyl groups in dextran, this polysaccharide is highly water soluble and thus a potential candidate to form ABS. Indeed, this polymer is commonly used on polymer-polymer ABS formulations[58]. However, despite its potential to be used as a two-phase inducer in aqueous media, no studies using dextran for forming IL-based ABS were hitherto found.

Regarding the potential ability of dextran to create ABS, in this work, novel biphasic systems composed of several dextrans, of different molecular weights, and diverse phosphonium-based ILs were investigated aiming at finding more profitable and sustainable liquid-liquid extraction approaches. In fact, the use of carbohydrates to replace the typical highly charged systems IL-based ABS[8] might lead to improved biotechnological routes. In particular, the ternary phase diagrams, tie-lines and tie-line lengths for 3 dextrans (M_w = 6,000, 40,000 and 100,000 Da) and 4 phosphonium-based ILs were determined at 298 K and atmospheric pressure.

To further address the potential of the studied systems as alternative extractive approaches, they were additionally evaluated for the extraction of three amino acids (L-tyrosine, L-tryptophan and L-phenylalanine). Tyrosine (4-hydroxyphenylalanine) is one of the 20 amino acids that are used to synthesize proteins. It is a non-essential amino acid because it can be synthesized from phenylalanine. In contrast to chemical production, biotechnological methods can produce L-tyrosine from biomass feedstock under environmentally-friendly and near carbon-free conditions[72]. Phenylalanine is an essential amino acid, classified as nonpolar because of the hydrophobic nature of the benzyl side chain. This amino acid is used in the manufacture of food products and sold as a nutritional supplement for its reputed analgesic and antidepressant effects[72]. Tryptophan is also an amino acid industrially produced by fermentation and is essential in the human diet. The distinguishing structural characteristic of tryptophan is the indole

functional group[73]. The molecular structures of the three amino acids studied are depicted in Figure 8.

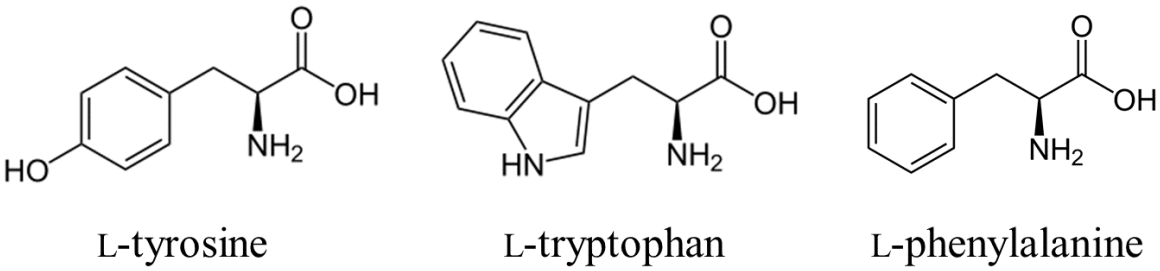

Figure 8. Amino acids chemical structures: L-tyrosine, L-tryptophan and L-phenylalanine.

Amino acids were selected as the partitioning solutes since they are very important biochemical products within a market which is growing due to the increasing demand for amino-acid-based dietary supplements. The high demand for aromatic amino acids is mainly due to their importance as nutrients and flavorings for food or feed industries, and as starting materials for pharmaceuticals, cosmetics and other chemicals.

The conventional techniques used for the separation of amino acids includes ionic exchange, reversed micelle methods and liquid-membrane extraction processes[8]. Most of these processes require the use of organic solvents with all their inherent problems, such as high flammability and toxicity. The key to recover high purity amino acids from fermentation broths relies on the selection of adequate separation and purification techniques. An economically feasible recovery of amino acids from the fermentation broth requires: (i) simple recovery; (ii) high recovery yield; (iii) minimum process steps; and (iv) easy process able to scale-up[72]. Therefore, the novel ABS proposed in this section were also investigated to ascertain on their potential to extract amino acids.

2.2 Experimental Section

IL-based ABS appear as promising separation processes since they provide efficient extractions while maintaining a suitable aqueous environment for biomolecules. Most of those systems focused on imidazolium-based ILs combined with inorganic salts[8]. This work intends to fill the gap in the study of phosphonium-based ILs and introduces new polysaccharides to form ABS.

A set of phosphonium-based ILs (combinations between different cations and anions) was studied aiming at obtaining new insights regarding their ability toward the formation of ABS and their competence for the extraction of amino acids.

2.2.1 Materials

Dextran from *Leuconostoc spp*., $(C_6H_{10}O_5)_n$, was supplied from Sigma-Aldrich. Three dextrans of different average molecular weights were used, namely dextran *of* 6,000 $g \cdot mol^{-1}$, 40,000 $g \cdot mol^{-1}$, and 100,000 $g \cdot mol^{-1}$ (and referred hereinafter as 6 kDa, 40 kDa and 100 kDa). The chemical structure of dextran was previously presented in Section 1.3.2 in Figure 7.

The ILs investigated were phosphonium-based, namely ethyl(tributyl)phosphonium diethylphosphate, $[P_{4442}][Et_2PO_4]$ > 95.0 wt % pure, tetrabutylphosphonium bromide, $[P_{4444}]Br$ > 96.0 wt % pure, tetrabutylphosphonium chloride, $[P_{4444}]Cl$ > 96.0 wt % pure, triisobutyl(methyl)phosphonium tosylate, $[P_{i(444)1}][Tos]$ > 99.0 wt % pure, tributyl(methyl)phosphonium methylsulfate, $[P_{4441}][MeSO_4]$ > 98.6 wt % pure, and tributyl(tetradecyl)phosphonium chloride, $[P_{444(14)}]Cl$ > 97.0 % pure. All ILs were kindly supplied by CYTEC Industries, Inc. All the molecular structures and the respective designations of the ILs studied are presented in Figure 9. As some ILs, namely $[P_{4444}]Br$ and $[P_{4444}]Cl$, presented excessive water content, individual samples of each ionic liquid were dried at moderate temperature (≈ 323 K) and high vacuum (≈ 10^{-5} Pa), under constant stirring for a minimum of 72 hours, in order to reduce the water and volatile compounds content to negligible values. The

purity of each ionic liquid was additionally verified by ^{1}H and ^{13}C and ^{31}P NMR assays.

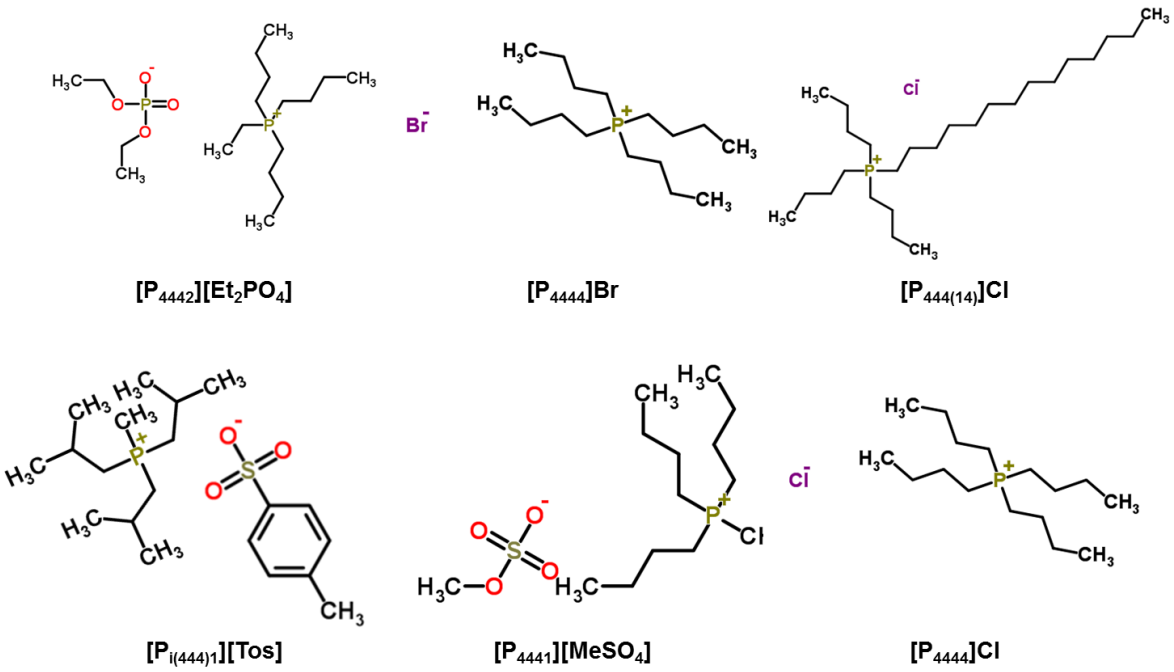

Figure 9. Chemical structure of the studied phosphonium-based ionic liquids.

The amino acids used as partitioning solutes were: L-tyrosine, $C_9H_{11}NO_3$ > 99.0 wt % pure from Sigma-Aldrich; L-tryptophan, $C_{11}H_{12}N_2O_2$ > 99.0 wt % pure from Fluka; and L-phenylalanine, $C_9H_{11}NO_2$ > 99.0 wt % pure from Merck.

Ethanol absolute, 99.5%, used for the polysaccharide precipitation was supplied by Fisher Scientific Chemicals.

The water used was distilled twice, passed by a reverse osmosis system and further treated with a Milli-Q plus 185 water purification apparatus.

2.2.2 Experimental Procedure

2.2.2.1 Phase Diagrams and Tie-Lines

Aqueous solutions of 40 wt % dextran (6 kDa, 40 kDa and 100 kDa) were initially prepared for the phase diagrams determination. ILs were used pure

whenever liquid at room temperature, or in aqueous solutions (80 to 90 wt %) when they are solid at the same conditions. All the solutions were prepared by weight (± 10^{-4} g) using an analytical balance, Mettler TOLEDO Excellence, XS205 Dual Range. All the aqueous solutions were further homogenized with a VWR™ International Vortex, VV3.

The binodal curves were determined at room temperature (298 ± 1) K and at atmospheric pressure through the cloud point titration method[74]. As Figure 10 outlines, the procedure consists on the repetitive drop-wise addition of each IL (pure or aqueous solution) to the aqueous dextran solution under constant stirring until the cloud point is reached (which means a biphasic region). After this step, the drop-wise addition of water is carried out until revealing a clear and limpid solution (which means that the monophasic region was attained). This procedure was carried out consecutively until a low dextran concentration is reached in the overall solution (about 5 wt %). The weight fraction compositions were determined gravimetrically within ± 10^{-4} g. The experimental procedure here adopted was previously validated by us[75] for ABS constituted by imidazolium-based ILs and dextran.

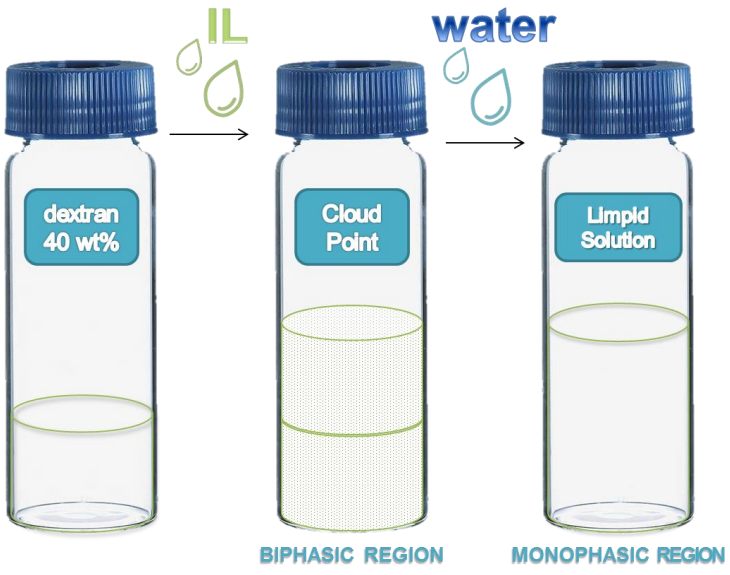

Figure 10. Schematic representation of the cloud point titration method.

The experimental binodal data were fitted through an empiric correlation previously proposed by Merchuk et al.[29] to describe polymer-based systems and according to Equation 1,

$$[IL] = Aexp[\ (B[dextran]^{0.5}) - (C[dextran]^3)\ ] \quad (1)$$

where [*IL*] and [*dextran*] are, respectively, the IL and dextran weight fraction percentages; and the coefficients *A*, *B* and *C* are the parameters obtained by the regression of the experimental data.

The tie-lines (TLs) were obtained by the determination of the amount of each component at the coexisting phases: different amounts of IL, dextran and water were used to prepare mixtures with rigorous compositions previously chosen and at the biphasic region. The prepared solutions were vigorously stirred on vortex (VWR™ International Vortex, VV3) and then centrifuged (Thermo Scientific, HERAEUS Megafure 16R) for 1 h at 3500 rpm and at controlled temperature (298 ± 1) K. Through this process the system undergoes the equilibrium by the separation into two different phases, which were further carefully separated and weighted.

Each TL was then obtained by a quantitative analysis of the exact concentration of each compound on both phases. Both the top and bottom phases were analyzed. Dextran was quantified by dry weight after precipitation with ethanol. Both phases were separated and to each one (*circa* 1 g) it was added ethanol (w:w = 1:1) to precipitate dextran. The samples were vortexed and then centrifuged at 3500 rpm and 298 K for 30 min. The ethanol rich upper liquid phase was then removed and dextran was additionally twice washed with ethanol at the same proportions. Ethanol was finally evaporated in an air oven at constant temperature (± 333 K) for at least 48 h. The amount of dextran at each phase was determined gravimetrically until constant weight. This procedure was previously optimized with a known amount of dextran (*circa* to 0.60 g) in aqueous solution (*circa* to 4.40 g of water) with recovery efficiencies in the order of (94 ± 3) % (result of 4 individual precipitation tests). The water content in each phase was determined by evaporation until constant weight of the dried IL + dextran in an air

oven and at constant temperature (± 333 K). The water content in each phase was also determined using a Metrohm 831 Karl-Fischer coulometer to compare with the data given by evaporation. The analyte used for the coulometric Karl-Fischer titration was Hydranal – Coulomat AG from Riedel-de Haën. The ILs amount was finally quantified by weight difference. Each sample was analyzed in duplicated vials to ascertain on the associated standard deviations.

The TLL, calculated through Equation 2, also provides important information to characterize the ABS,

$$TLL = \sqrt{([dextran]_T - [dextran]_B)^2 + ([IL]_T - [IL]_B)^2} \qquad (2)$$

where *T* represents the top phase and *B* the bottom phase, [dextran] and [IL] are the weight fraction of the dextran- and the IL-rich phases, respectively. In all the studied systems the bottom phase is the dextran-rich phase whereas the top layer is enriched in IL.

2.2.2.2 Extraction of Amino Acids

Aqueous solutions of L-tyrosine (0.37 g·dm^{-3}), L-tryptophan (0.76 g·dm^{-3}) and L-phenylalanine (7.00 g·dm^{-3}), were prepared for the studies on the amino acids partitioning. At these concentrations, the complete solubility in water was verified for each amino acid.

All the partitioning studies were performed at a constant mixture composition: 35 wt % IL + 15 wt % dextran + 50 wt % amino acid aqueous solution. This composition was chosen based on the phase diagrams previously determined for each IL/dextran combination. The ternary mixture compositions were gravimetrically prepared within ± 10^{-4} g. Once fully dissolved by stirring, mixtures were centrifuged for 1 h at 3500 rpm and (298 ± 1) K to achieve the complete partitioning of each amino acid between both aqueous phases. The two phases were carefully separated using disposable plastic syringes and the amino acid concentration was quantified in each phase by UV-spectroscopy, carried out with a SHIMADZU UV-1700, Pharma-Spec Spectrometer, at a wavelength of 275 nm for

L-tyrosine, 279 nm for L-tryptophan and 257 nm for L-phenylalanine. Calibration curves were previously established for each individual compound (*cf*. Appendix B). Blank control samples were always used and values for at least three replicated samples of each system were quantified in order to determine the average in the amino acids partition coefficients and the corresponding standard deviations.

The partition coefficients of each amino acid (K_{AA}) are defined as the ratio of the concentration of each amino acid in the IL-rich (top) phase and in the dextran-rich (bottom) phase, as described by Equation 3,

$$K_{AA} = \frac{[AA]_T}{[AA]_B} \quad (3)$$

where $[AA]_T$ and $[AA]_B$ are, respectively, the concentrations of amino acid in the top and in the bottom phases.

The extraction efficiencies of each amino acid (EE_{AA}%) are defined as the percentage ratio between the amount of AA in the IL-rich aqueous phase and that amount in the total mixture, as defined in Equation 4,

$$EE_{AA}\% = \frac{[AA]_T \times w_T}{([AA]_T \times w_T + [AA]_B \times w_B)} \times 100 \quad (4)$$

where $[AA]_T$ and $[AA]_B$ are respectively the amount of amino acid in the top and in the bottom phases, and w_T and w_B are the weight of each phase.

2.3 Results and Discussion

2.3.1 Phase Diagrams and Tie-Lines

In this work both the effects of the IL chemical structure and the polysaccharide molecular weight were evaluated in what concerns the phase separation ability and further creation of ABS. Since they are novel systems, the first step of this study comprises the determination of the respective phase diagrams. The binodal curves, and respective TLs and TLLs, were determined at 298 K and atmospheric pressure and are here presented for each IL-dextran combination.

From the ILs studied in this work, $[P_{i(444)1}][Tos]$, $[P_{4441}][MeSO_4]$, $[P_{444(14)}]Cl$ and $[P_{4444}]Br$ are able to form ABS with the three dextrans investigated (M_w = 6,000, 40,000 and 100,000 Da). The respective ternary phase diagrams are displayed in Figures 11 to 13 where the effect of the IL to undergo liquid-liquid demixing can be appraised. However, it should be remarked that it was not detected the formation of ABS with $[P_{4444}]Cl$ or $[P_{4442}][Et_2PO_4]$ independently of the dextran molecular weight.

All data in this section are displayed in weight percentage (wt %) and in molality units ($mol \cdot kg^{-1}$), moles of solute *per* kg of solvent) for a better perception of the distinct potential for phase formation avoiding thus inconsistencies that may result from the various molecular weight variations of the solutes. The experimental weight fraction data for all the systems are available in Appendix A.

The binodal curves depicted in Figures 11 to 13 provide information regarding the minimum concentration of the phase forming components required to form a two-phase system. All the presented diagrams have a vertical axis for the IL-enriched phase, which is the less dense (later referred as top) phase, and a horizontal axis for the dextran-enriched (bottom) phase. Every mixture with compositions above the coexistence binodal curve undergoes liquid-liquid demixing being within the biphasic region. A binodal closer to the origin axis results in a larger biphasic region.

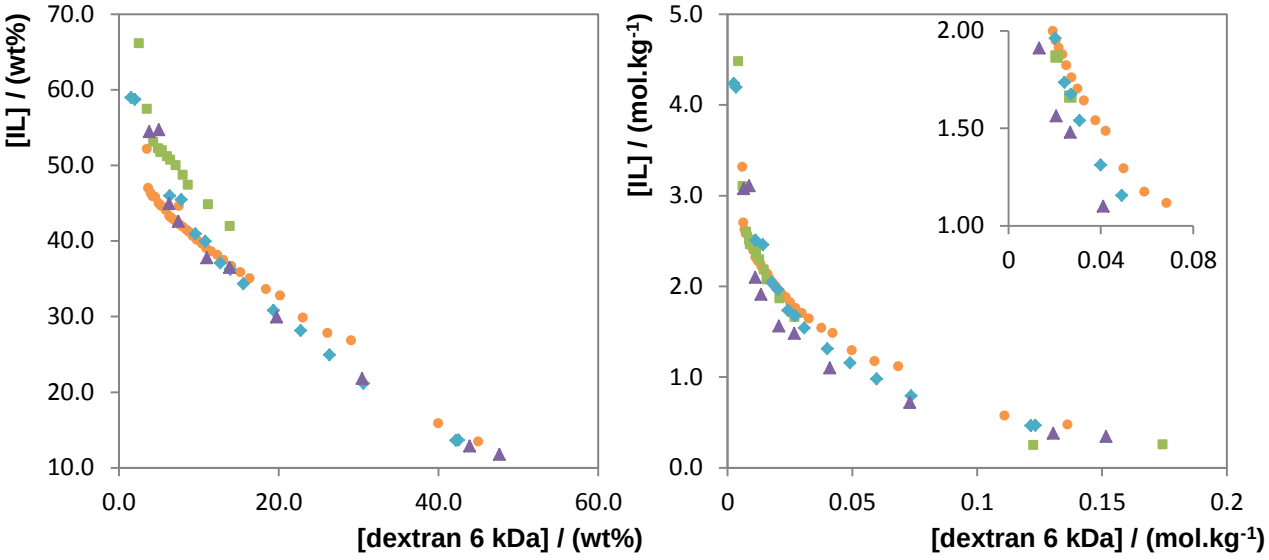

Figure 11. Phase diagrams for ternary systems composed of IL + dextran 6 kDa + H_2O at 298 K : ▲, $[P_{i(444)1}][Tos]$; ●, $[P_{4441}][MeSO_4]$; ■, $[P_{444(14)}]Cl$; ◆, $[P_{4444}]Br$ (left: wt%; right: mol.kg^{-1}).

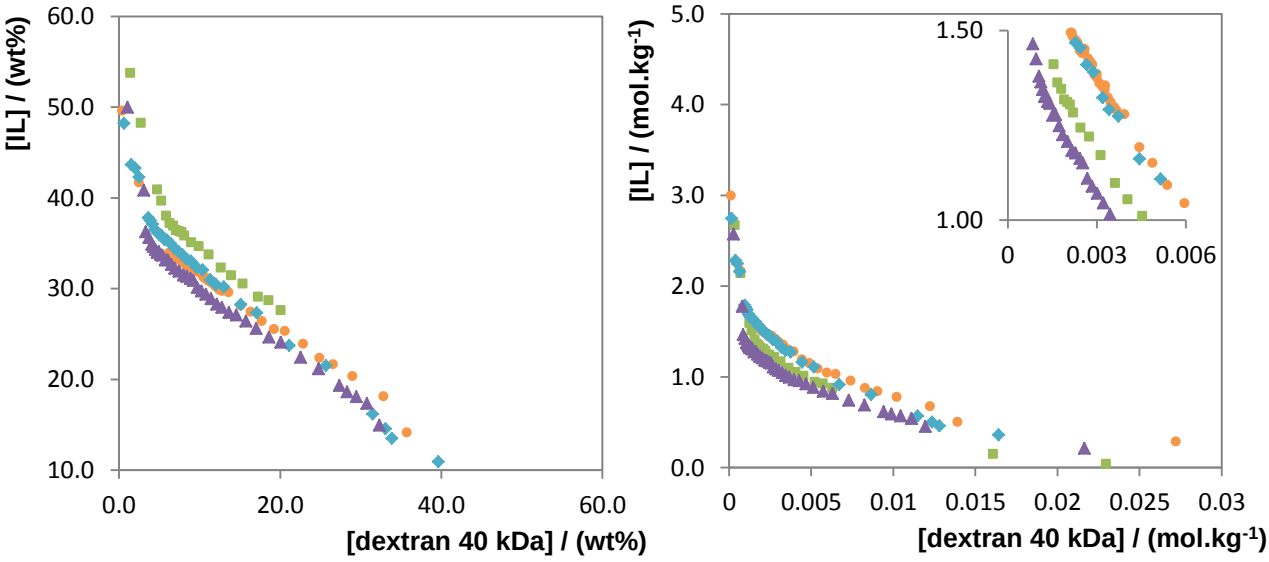

Figure 12. Phase diagrams for ternary systems composed of IL + dextran 40 kDa + H_2O at 298 K: ▲, $[P_{i(444)1}][Tos]$; ●, $[P_{4441}][MeSO_4]$; ■, $[P_{444(14)}]Cl$; ◆, $[P_{4444}]Br$ (left: wt%; right: mol.kg^{-1}).

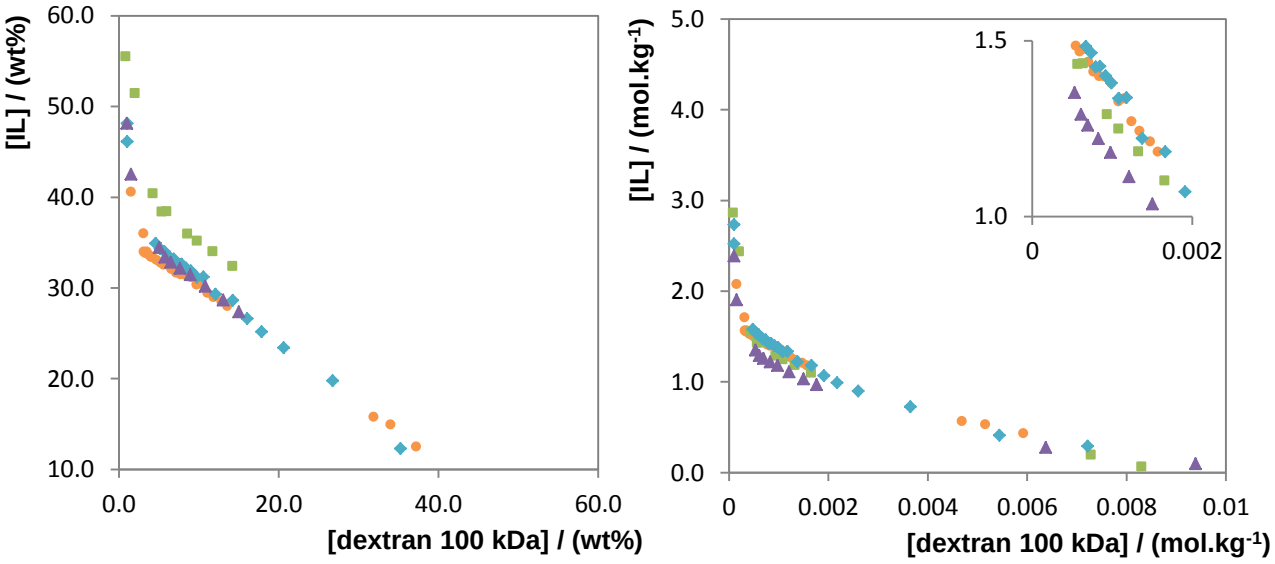

Figure 13. Phase diagrams for ternary systems composed of IL + dextran 100 kDa + H_2O at 298 K : ▲, $[P_{i(444)1}][Tos]$; ●, $[P_{4441}][MeSO_4]$; ■, $[P_{444(14)}]Cl$; ◆, $[P_{4444}]Br$ (left: wt%; right: mol.kg^{-1}).

The obtained results show that there are small, but still perceptible, quantitative differences in the binodal curves of the phosphonium-based ILs. The ability of the ILs to form ABS follow the order: $[P_{i(444)1}][Tos]$ > $[P_{444(14)}]Cl$ > $[P_{4444}]Br$ > $[P_{4441}][MeSO_4]$, while $[P_{4444}]Cl$ does not form ABS. Thus, for the same dextran concentration, $[P_{i(444)1}][Tos]$ and $[P_{4441}][MeSO_4]$ present, respectively, the higher and the lower ability to induce phase separation in ternary systems composed of IL + dextran + H_2O, whereas $[P_{4444}]Cl$, being one of the most hydrophilic ILs investigated, is not salted-out by dextran.

The higher the hydrophilic nature of the IL the lower is its ability to form ABS. This results means that more hydrophobic ILs are more easily excluded for a second liquid phase and that dextrans seem to behave as salting-out agents. The quaternary phosphonium cations in the studied ILs present four alkyl chains which are responsible for their lower affinity for aqueous phases and it is known that the hydrophobicity is increased for long alkyl chains. For this reason, $[P_{444(14)}]Cl$ can form an ABS while $[P_{4444}]Cl$ does not. However, their water miscibility is mainly due to the polar water hydrogen-bonding with the IL anions. Studies regarding

empirical polarity scales based on solvent interactions with a reference solute lead to a rank on the compounds, providing useful information on the IL cations and anions solvation at the molecular level[37]. Reichardt reviewed the empirically polarity of room-temperature ILs by means of betaine dye[76]. Previously it was demonstrated that the formation of ABS with imidazolium-based ILs is closely correlated with the β (hydrogen-bond basicity or ability to accept protons) values of their anions[77]. The β values are mainly dependent on the IL anion and for 1-butyl-3-methylimidazolium-based ILs they follow the rank: Cl^- (0.95)[78] > Br^- (0.87)[79] > $[MeSO_4]^-$ (0.67)[80]. Therefore, amongst the three IL anions, chloride is the more able to accept protons from water, resulting in a higher affinity for water, and the less able to form an ABS if a similar cation is present. On the other hand, the $[MeSO_4]$-based IL should be more able to create an ABS than the Br-based IL according to the hydrogen-bond basicity scale. Nevertheless, the respective cation presents an alkyl chain with a shorter length and thus a higher affinity for water. In summary, both the cation and the anion of the IL contribute for the ability of ABS formation. Finally, the large aromatic ring in $[P_{i(444)1}][Tos]$ enhances the IL aptitude to undergo liquid-liquid demixing and this is in close agreement with the phase diagrams behavior composed of imidazolium-based ILs and where this anions usually leads to larger biphasic regions[81].

The tunable character of the ternary systems phase behavior is not exclusively derived from the manipulation of the IL chemical structure. In fact, dextran also provides the opportunity of design by the choice of the average molecular weight, and the length of its polymeric chains. Figures 14 to 17 depict the binodal curves for each IL evaluated, varying the average dextran molecular weight from 6 kDa to 100 kDa. The experimental weight fraction data of each phase diagram are given at Appendix A.

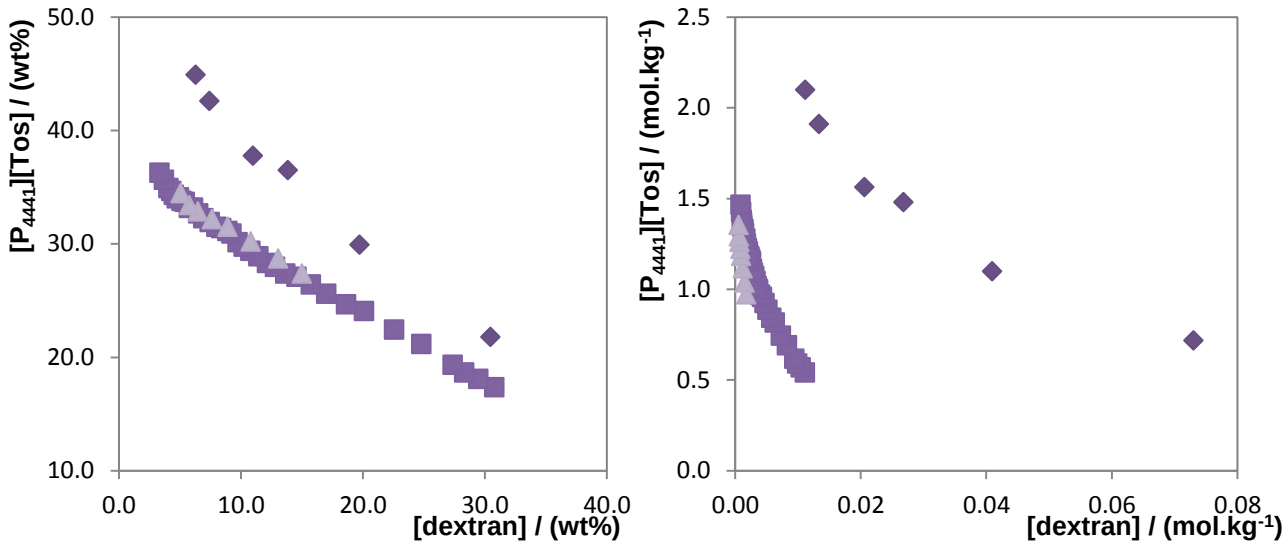

Figure 14. Phase diagrams for ternary systems composed of $[P_{i(444)1}][Tos]$ + dextran + H_2O at 298 K: ◆, dextran 6 kDa; ■, dextran 40 kDa; ▲, dextran 100 kDa (left: wt%; right: mol.kg^{-1}).

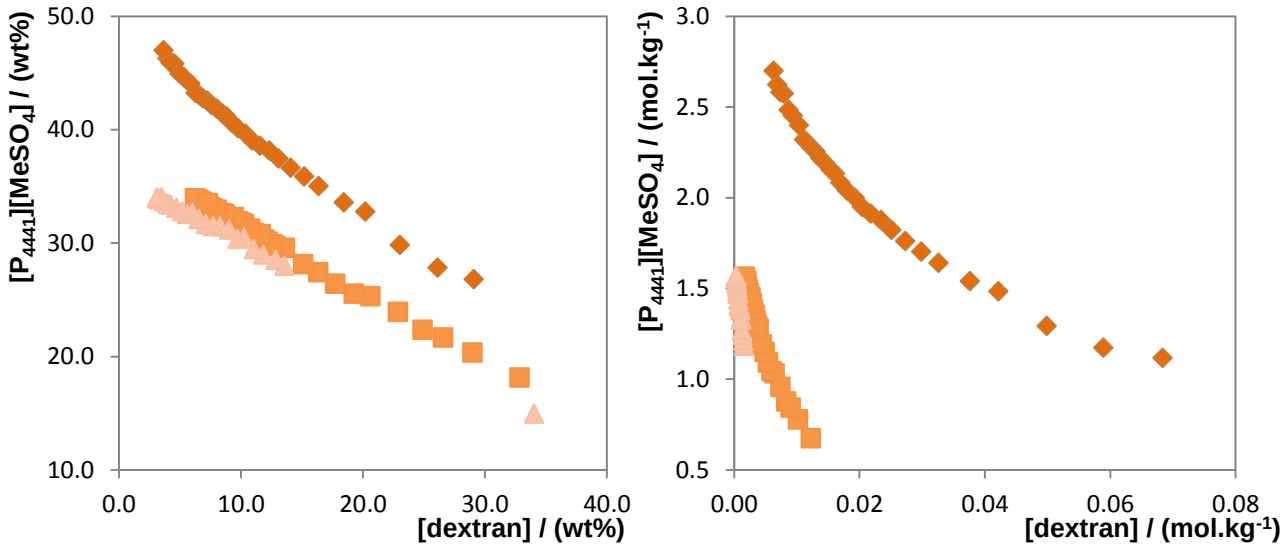

Figure 15. Phase diagrams for ternary systems composed of $[P_{4441}][MeSO_4]$ + dextran + H_2O at 298 K: ◆, dextran 6 kDa; ■, dextran 40 kDa; ▲, dextran 100 kDa (left: wt%; right: mol.kg^{-1}).

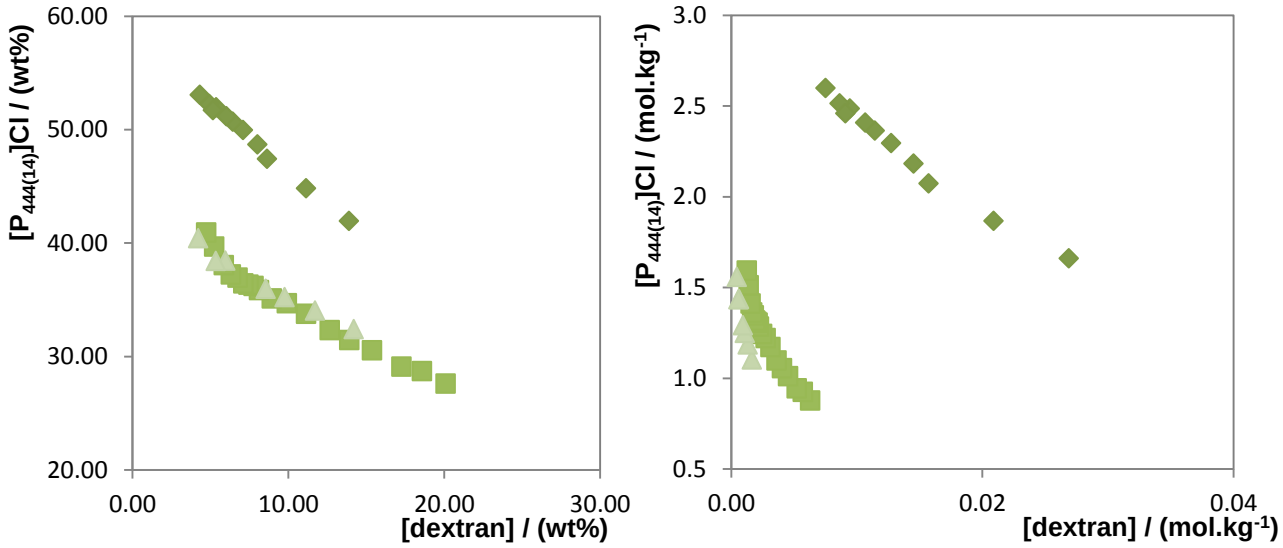

Figure 16. Phase diagrams for ternary systems composed of $[P_{444(14)}]Cl$ + dextran + H_2O at 298 K: ◆, dextran 6 kDa; ■, dextran 40 kDa; ▲, dextran 100 kDa (left: wt%; right: mol.kg^{-1}).

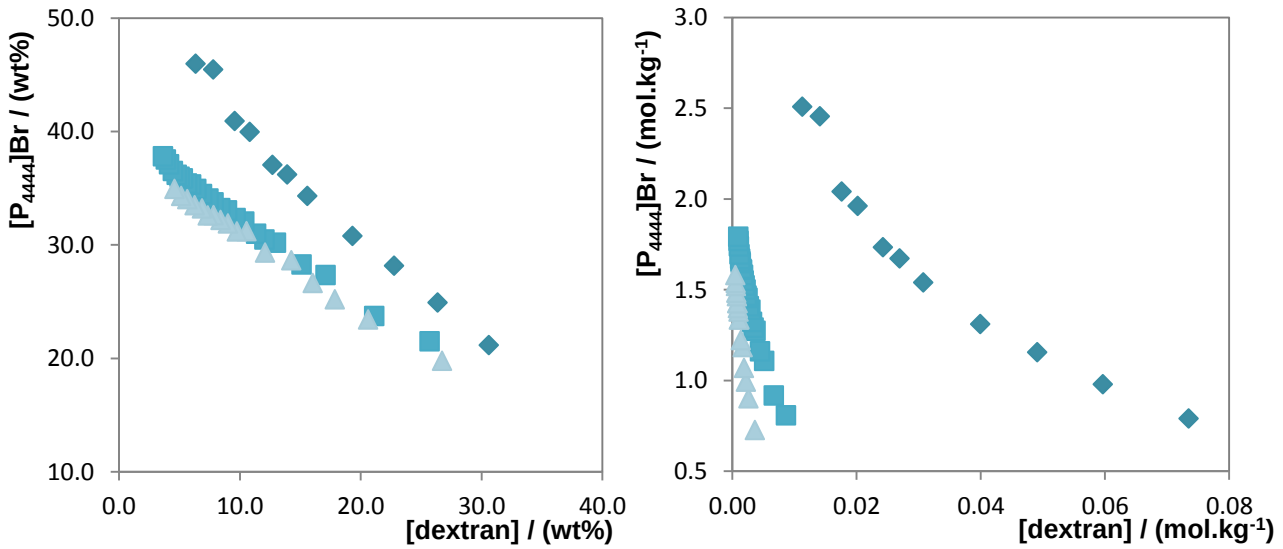

Figure 17. Phase diagrams for ternary systems composed of $[P_{4444}]Br$ + dextran + H_2O at 298 K: ◆, dextran 6 kDa; ■, dextran 40 kDa; ▲, dextran 100 kDa (left: wt%; right: mol.kg^{-1}).

From the presented results, it can be seen that, for a common IL and independently of the IL, a variation in the average molecular weight influences the phase separation. The ability of dextran to induce IL-based ABS follows the order: dextran 100 kDa > dextran 40 kDa > dextran 6 kDa. The same trend was observed in a previous work for systems composed of imidazolium-based ILs + dextran + water[75]. Also in accordance, it was previously reported that polymers with higher molecular weight are preferentially segregated from ionic liquids[8]. Furthermore, Freire et al.[38], based on the experimental data of ternary systems constituted by ILs, water and mono- and disaccharides, as well as polyols, concluded that two main factors are subjacent to the carbohydrates' salting-out aptitude: (i) the number of -OH groups, and (ii) the corresponding intrinsic stereochemistry. In fact, dextran contains a large number of –OH groups, is an H-bond acceptor and its molecules have the ability to form hydrogen bonds with water, a protic solvent, being this interaction highly responsible for the dextran water solubility[82]. Hence, an increase in the dextran molecular weight, and the consequent increase in the number of –OH groups *per* mole, may lead to a more extensive formation of complexes with water, although a linear relationship between molecular weight and hydrogen-bonding may not be rigorously observed due to the polymer branching[83]. The solubility curves experimentally determined for the two dextran types of higher molecular weight (40 kDa and 100 kDa) are almost coincidental, regardless of the IL they are combined with. This seems to demonstrate that not only the number of –OH groups *per* unit mass but also the conformation and the intra- and inter-hydrogen-bonding is identical for both dextran types of molecules. The solubility data for dextran 6 kDa reveal that it has a lower ability to promote phase splitting, since a comparatively higher mass fraction is needed for all ILs studied (*cf*. Appendix A). This is an unexpected result, considering that the number of -OH groups *per* mass unit should be the same and hence lead to similar solubility data. The discrepancy may stem from the different conformation of dextran 6 kDa; in water, dextran fractions behave as flexible and extended polymers, with dextran 6 kDa having the conformation of an expandable coil and dextrans 40 kDa and 100 kDa being more symmetric,[71] and with higher branching degree[83]. The intrinsic viscosity of dextrans, although dependent of the

branched linkage pattern[84] and of the conformation of their molecules,[71] increases with the polysaccharide molecular weight and respective concentration. That parameter is a measure of the effective hydrodynamic volume of the polymer in solution[85] and reflects the hydrogen-bonding, dipole-dipole and hydrophobic interactions with the solvent[82, 86]. However, since the degree of solubility in water decreases with the increase of the degree of branching, dextran 40 kDa and 100 kDa, being more branched, may present a lower solubility value[87].

The experimental binodal curves were fitted to the empirical correlation described by Merchuk et al.[29] (Equation 1). The regression parameters, the coefficients *A*, *B* and *C*, and the corresponding standard deviation and correlation coefficient (*sd* and R^2) were estimated by least squares regression for each ternary system and are reported in Table 1. Overall, satisfactory correlation coefficients were obtained and the corresponding parameters are most useful to predict data in a given region of the phase diagram where no experimental data are available.

As an example, Figure 18 evidences that the empirical Equation 1 satisfactorily correlates the experimental data for the system composed of $[P_{4444}]Br$ + dextran 40 kDa + H_2O. The same behavior is consistently observed for the remaining investigated systems. However, unlike many of the works reported in this field[8], the compositions of the ternary systems at equilibrium, namely the TLs, were not solely determined by the lever-arm rule as proposed by Merchuk et al.[29]. Instead, they were experimentally determined by quantitative analysis. An example of the TLs obtained is also shown in Figure 18, for the ternary system composed of $[P_{4444}]Br$ and dextran 40 kDa. In general, the TLs for each system are closely parallel.

Table 1. Adjusted parameters used to describe the experimental binodal data for the phosphonium-based ILs + H_2O + dextran systems by Equation 1.

IL + Dextran + H_2O	*A*	*B*	10^5 *C*	R^2	100 sd [a]
$[P_{i(444)1}][Tos]$					
dextran 6 kDa	86.8262	-0.2406	0.3178	0.9849	0.9806
dextran 40 kDa	51.7506	-0.1721	0.5588	0.9632	0.9612
dextran 100 kDa	54.6076	-0.1839	1.0455	0.9873	0.9845
$[P_{4441}][MeSO_4]$					
dextran 6 kDa	60.8606	-0.1294	0.7152	0.9864	0.9855
dextran 40 kDa	52.7037	-0.1608	0.4630	0.9872	0.9867
dextran 100 kDa	42.5792	-0.1082	1.0938	0.9812	0.9796
$[P_{444(14)}]Cl$					
dextran 6 kDa	83.2737	-0.1936	0.8016	0.9806	0.9776
dextran 40 kDa	63.6714	-0.1903	1.6822	0.9819	0.9797
dextran 100 kDa	64.7585	-0.1952	1.3572	0.9839	0.9799
$[P_{4444}]Br$					
dextran 6 kDa	76.1824	-0.1955	0.6045	0.9980	0.9977
dextran 40 kDa	52.4372	-0.1556	0.9687	0.9910	0.9904
dextran 100 kDa	54.3066	-0.1777	0.7964	0.9819	0.9799

[a] $sd = \left(\sum_{i=1}^{n} \left(w_{IL}^{cal} - w_{IL}^{exp} \right)^2 / n \right)^{0.5}$, where w_{IL}^{exp} is the experimental weight fraction of IL (described in Appendix A), w_{IL}^{cal} is the corresponding data calculated using Equation 1 and n represents the number of binodal data points.

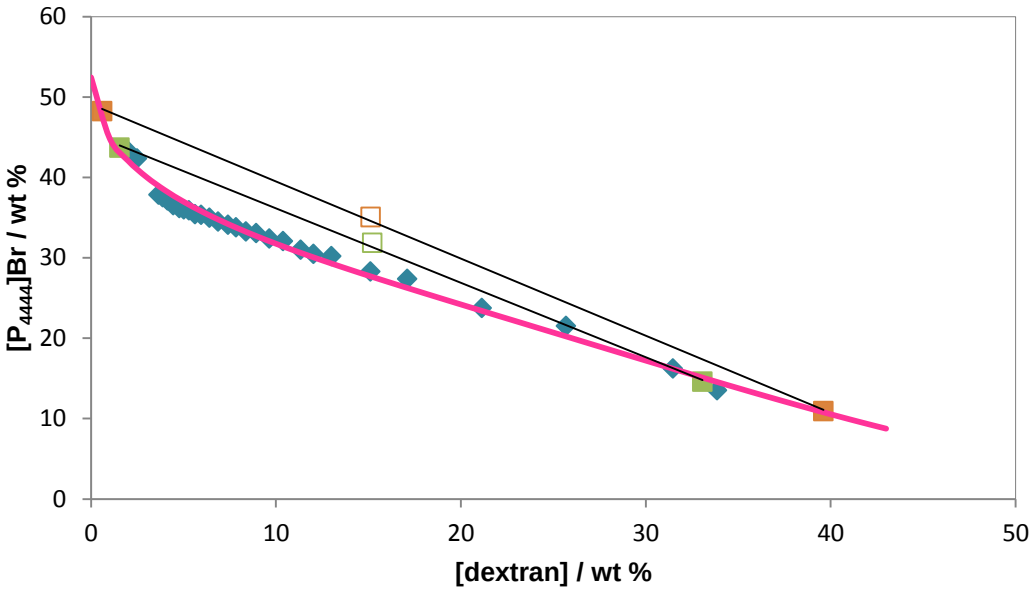

Figure 18. Phase diagrams for the $[P_{4444}]Br$ + dextran 40 kDa + H_2O ternary system at 298 K: ◆, Experimental data; ─, fitting by eq.1; ■, TL 1; ■, TL 2.

The weight fraction compositions for the coexisting phases (TLs) alongside their respective length (TLL) of all systems are reported in Table 2. Since the TLL represents the difference between the IL and the dextran concentrations in the top and bottom phases, respectively, the larger the TLL, the more complete is the IL and the dextran partitioning resulting in a top IL-enriched and a bottom dextran-enriched phase.

Table 2. Weight fraction compositions of the coexisting phases and respective values of α and TLL.

IL + dextran + H_2O		weight fraction composition / wt %				
		$[dextran]_T$	$[IL]_T$	$[dextran]_B$	$[IL]_B$	TLL
$[P_{i(444)1}][Tos]$						
dextran 6 kDa	TL1	3.77	54.43	43.91	12.84	57.81
	TL2	4.97	54.68	47.63	11.78	60.50
dextran 40 kDa	TL1	1.04	49.98	46.40	7.72	61.99
	TL2	3.09	40.83	32.33	14.96	39.04
dextran 100 kDa	TL1	1.50	42.54	38.93	9.78	49.74
	TL2	0.99	48.14	48.43	3.80	64.93
$[P_{4441}][MeSO_4]$						
dextran 6 kDa	TL1	3.49	52.12	44.97	13.46	56.71
	TL2	7.51	44.58	39.98	15.88	43.34
dextran 40 kDa	TL1	2.50	41.69	35.74	14.16	43.16
	TL2	0.42	49.60	52.11	8.60	65.98
dextran 100 kDa	TL1	1.50	40.60	37.21	12.52	45.42
	TL2	3.06	36.01	31.90	15.79	35.22
$[P_{444(14)}]Cl$						
dextran 6 kDa	TL1	2.50	66.09	51.11	9.98	74.24
	TL2	3.50	57.43	42.36	9.75	61.51
dextran 40 kDa	TL1	2.73	48.25	39.13	6.18	55.63
	TL2	1.39	53.77	47.87	1.70	69.79
dextran 100 kDa	TL1	1.99	51.47	45.36	2.90	65.12
	TL2	0.80	55.51	42.13	7.92	63.03
$[P_{4444}]Br$						
dextran 6 kDa	TL1	1.49	58.97	42.17	13.62	60.92
	TL2	2.00	58.72	42.52	13.68	60.58
dextran 40 kDa	TL1	1.99	43.29	33.85	13.50	43.62
	TL4	0.60	48.23	39.61	10.93	53.98
dextran 100 kDa	TL1	1.00	46.15	35.24	12.32	48.13
	TL2	1.00	48.13	41.92	9.13	56.53

2.3.2 Extraction of Amino Acids

The partition studies of amino acids, as protein monomers, in ABS, have great significance in the improvement of purification techniques which can later be extended to proteins or even enzymes. Although there are several works in the literature reporting IL-based ABS for the extraction of amino acids[17, 37, 88-91], the present work is pioneering in substituting the common used salts by polysaccharides.

Table 3. Partition coefficients and extraction efficiency values of L-tyrosine, L-tryptophan and L-phenylalanine in the ternary system composed of 35 wt % IL + 15 wt % dextran 40 kDa + 50 wt % H_2O at 298 K.

IL	AA	weight fraction composition / wt %		EE_{AA} %	*K*
		$[IL]_M$	$[dextran]_M$		
$[P_{4441}][MeSO_4]$	tyrosine	35.03	15.12	85.59	2.64
		35.07	15.11	86.52	2.79
		34.99	15.09	87.15	2.79
		35.03	15.11	86.42	2.74
	tryptophan	35.00	15.00	88.45	3.17
		35.07	15.03	85.02	2.62
		34.97	15.00	84.82	2.49
		35.01	15.01	86.10	2.76
	phenylalanine	34.95	15.02	76.81	1.52
		34.93	15.01	87.44	3.16
		35.03	14.98	74.36	1.19
		34.97	15.01	79.54	1.96
$[P_{4444}]Br$	tyrosine	34.93	14.98	78.49	2.08
		34.84	14.94	78.11	2.10
		34.96	14.99	80.35	2.42
		34.91	14.97	78.98	2.20
	tryptophan	34.99	15.00	82.62	2.84
		34.91	14.97	81.87	2.56
		34.83	14.93	82.35	2.85
		34.91	14.97	82.28	2.75
	phenylalanine	34.93	14.97	71.28	1.46
		34.91	14.96	73.90	1.68
		34.86	14.94	71.72	1.52
		34.90	14.95	72.30	1.55

■ - average value

After the complete characterization of the novel IL-dextran ABS, they were further evaluated in what concerns their ability to extract amino acids, namely tyrosine, tryptophan and phenylalanine. In order to exclude deviations that could arise from the ternary mixture compositions, the partition experiments of the studied amino acids were accomplished at a common mixture composition: 35 wt % IL + 15 wt % dextran 40 kDa + 50 wt % H_2O. The results obtained with $[P_{4441}][MeSO_4]$ and $[P_{4444}]Br$ are depicted in Table 3 by the partition coefficients and extraction efficiencies for each amino acid studied.

In all systems a preferential partitioning of the amino acids for the IL-rich aqueous phase was verified. The corresponding extraction efficiencies are depicted in Figure 19. Salabat et al.[91] also employed aqueous two-phase systems composed of polyethylene glycol (PEG 6000) + salts + H_2O at 298.15 K, and verified that more hydrophobic amino acids have a greater affinity for the hydrophobic PEG-rich phase and, consequently, larger partition coefficients. In this work, the most hydrophobic phase is the IL-rich phase, and thus, a preferential migration of the amino acids for this layer is observed.

The partitioning of hydrophilic and aromatic solutes, such as amino acids, mainly depends on the nature of the IL used and on the IL-amino acid interactions. As it was previously shown in Figure 8, the three amino acids structures are very similar, each of them with an amine and a carboxyl group, and a substituent group that distinguishes each one of these compounds: Phe, C_6H_5-CH_2-; Tyr, OH-C_6H_4-CH_2-; and Trp, aromatic ring.

Both Tyr and Trp, shown a similar behavior regarding the potential for their separation with ABS composed of phosphonium-based ILs and dextran. On the other hand, Phe is the amino acid which presents a lower extraction efficiency with both IL-based systems. The work from Zafarani-Moattar and Hamzehadeh[89] using ABS composed of ILs and salts reported that the behavior of different amino acids, at pH values close to their isoelectric points, decrease in the following order: $K_{Trp} > K_{Tyr} > K_{Phe}$. Although the study was performed with ABS composed of imidazolium-based ILs and salts, we found here the same trend in the phosphonium-dextran based systems investigated. In this work, the extraction efficiencies of all amino acids for the IL-rich phase are higher than 72 %. Therefore, it is possible to

replace the common used salts in the ABS composition without significant loss of efficiency in the extraction of amino acids. The partition coefficient obtained for amino acids in phosphonium-based IL ABS (e.g. K_{Trp} ≈ 2.75) is considerably higher than those obtained with PEG – polysaccharide systems (K_{Trp} ≈ 1)[92] and competitive with conventional PEG-inorganic salt systems (K_{Trp} ≈ 1-7)[91].

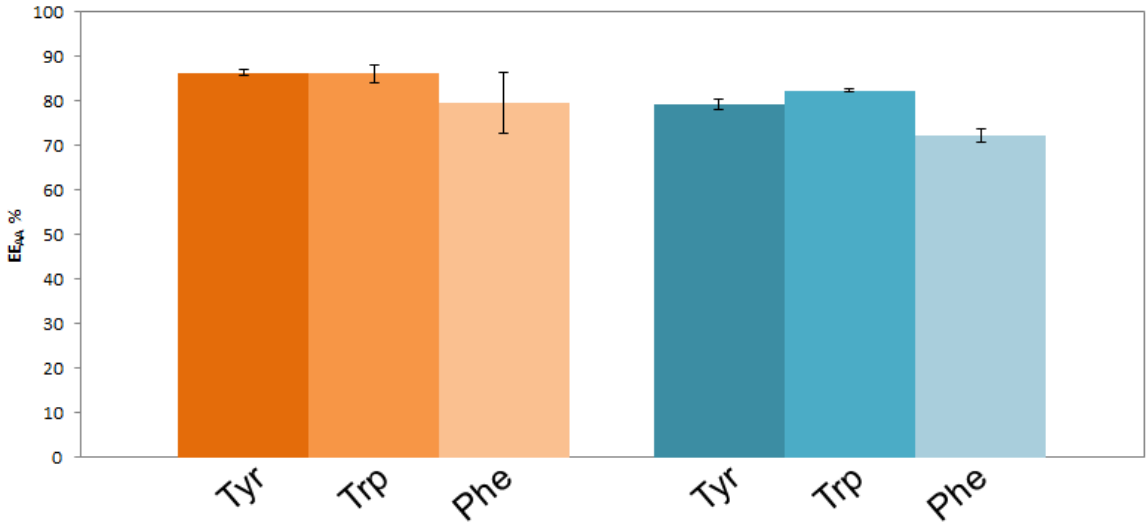

Figure 19. Percentage extraction efficiencies of each amino acid in ABS composed of 35 wt % IL + 15 wt % dextran 40 kDa + 50 wt % H_2O at 298 K: ■, $[P_{4441}][MeSO_4]$; ■, $[P_{4444}]Br$.

In contrast with the research focused on imidazolium-based ILs, Louros et al.[88] reported the extraction aptitude for amino acids of ABS composed of $[P_{1444}][MeSO_4]$ and K_3PO_4. The values of the partition coefficients obtained (K_{Trp} = 9.00)[88] are larger than those observed with the imidazolium-based ILs (K_{Trp} = 4.47)[37] and higher than the values obtained in this work. This result is a main consequence of the strong salting-out salt used by Louros et al.[88]. On the other hand, phosphonium-based fluids provide higher extraction efficiencies for hydrophobic substances and can be seen as a major advantage since these compounds present a higher thermal stability and do not have acidic protons, and are thus more stable compounds and valuable for specific applications over the imidazolium-based ones[8].

3 Phosphonium-based ILs + H_2O + maltodextrin

3.1 Introduction

Besides the dextran previously used, maltodextrin is another polysaccharide which could be of interest in ABS formulations. Maltodextrin is defined by the Food and Drug Administration (FDA)[93] as a mixture of nutritive carbohydrates, non-sweet, and with different degrees of polymerization. Maltodextrin is produced enzymatically from starch, corn-based in the US, but wheat-based in Europe. Maltodextrin is used in food industry applications, and in the paper or the pharmaceutical industries[59]. Maltodextrins have the ability to create the sensation of fat due to the tridimentional structure formed during their gellification process, and this makes them a most desired product to replace fat in food. [94]

According to Loret et al.[94], maltodextrins are the products obtained from starch, either by acid catalysis or enzymatically, that have dextrose equivalent values (DE) smaller than 20; those with higher values are classified as glycose syrup. These two classes of products, with DE above and below 20, have significant differences: the first are formed by small oligomers, freely soluble in water, but the later may contain a significant proportion of long polymeric chain polymers that may inhibit water solubilization and promote gellification. Maltodextrins are thus composed of high and low molecular weight polymers, with variable molecular weight and size, and are usually classified according to their DE value. The dextrose equivalent value is defined as the reducing sugar content of a known weight sample when compared to and equal weight of glucose (molecular weight of 180.16 $g.mol^{-1}$), that is given a DE value of 100 and may be related . The DE value is inversely proportional to the value of average molecular weight (M_w), as shown by the following expression,[95]

$$DE = \frac{100}{Mw/180.16} \quad (5)$$

To test the potentiality of maltodextrin as a new and alternative ABS inducer, the corresponding ternary phase diagrams for systems composed of different phosphonium-based ILs, water and two maltodextrins of different dextrose equivalents were determined at 298 K and atmospheric pressure. In addition, the

TLs and TLLs were also determined. The phase diagrams reveal the required information on the phase-forming compositions necessary to create an ABS.

3.2 Experimental Section

3.2.1 Materials

The same set of (hydrophilic) phosphonium-based ILs was used here and corresponds to those described in Section 3.2. In summary, the ILs investigated are $[P_{4442}][Et_2PO_4]$, $[P_{4444}]Br$, $[P_{4444}]Cl$, $[P_{i(444)1}][Tos]$, $[P_{4441}][MeSO_4]$ and $[P_{444(14)}]Cl$. Their chemical structures are shown in Figure 9. All ILs were generously supplied by CYTEC Industries, Inc., and have the same purity level and were subjected to the same purification procedure as previously described in Section 3.2.1.

Two maltodextrins of different dextrose equivalents (DE) were tested, namely 13.0-17.0 and 16.5-19.5, both supplied by Aldrich.

Ultra-pure water, double distilled, passed by a reverse osmosis system and further treated with a Milli-Q plus 185 water purification apparatus was used in all experiments.

3.2.2 Experimental Procedure

3.2.2.1 Phase Diagrams

For the phase diagrams determination, aqueous solutions of maltodextrin were prepared at *circa* 40 wt %. The ILs which are liquid at room temperature were used pure and the ILs which are solid at the same conditions were prepared in an aqueous solution at 90 wt%. The binodal phase diagrams were determined at room temperature (298 ± 1) K and at atmospheric pressure (≈ 1 atm) by the cloud point titration method[74]. The cloud point titration method corresponds to that previously described in Section 2.2.2.1. The experimental binodal curves were also fitted through Equation 1 previously described in Section 2.2.2.1.

3.3 Results and Discussion

In this work, the ability of maltodextrins to form ABS in the presence of ILs was evaluated for the first time. Novel ternary phase diagrams were determined at 298 K for each IL and each maltodextrin.

3.3.1 Phase Diagrams

The experimental phase diagrams were obtained at 298 K and atmospheric pressure for each IL + maltodextrin + H_2O system. The ILs $[P_{i(444)1}][Tos]$, $[P_{4441}][MeSO_4]$, $[P_{4442}][Et_2PO_4]$, $[P_{444(14)}]Cl$, $[P_{4444}]Br$ and $[P_{4444}]Cl$ combined with two maltodextrins of different dextrose equivalents (13.0-17.0 and 16.5-19.5 DE) were tested as phase-forming components of ABS. The weight fraction composition data corresponding to the binodal saturation curves are presented in Appendix A.

From the tested systems, $[P_{4442}][Et_2PO_4]$ and $[P_{4444}]Cl$ cannot form ABS with either the maltodextrins investigated. This inability of both ILs is consistent with the data previously shown with dextran and is again a direct result of these ILs higher hydrophilicity.

Figures 20 and 21 display the binodal curves for the systems which undergo phase separation and divided according to the type of maltodextrin used. All the phase diagrams are presented in weight fraction and in molality units to directly infer on their ability for two-phase formation independently of the IL molecular weight. Due to the absence of consistent molecular weight values for these polysaccharides, the average DE was determined for each maltodextrin and then converted to the molecular weight through the application of Equation 5. The obtained results reveal that the ability of ILs for ABS formation, and independently of the maltodextrin, follows the order: $[P_{444(14)}]Cl > [P_{4441}][MeSO_4] \approx [P_{4444}]Br > [P_{i(444)1}][Tos]$.

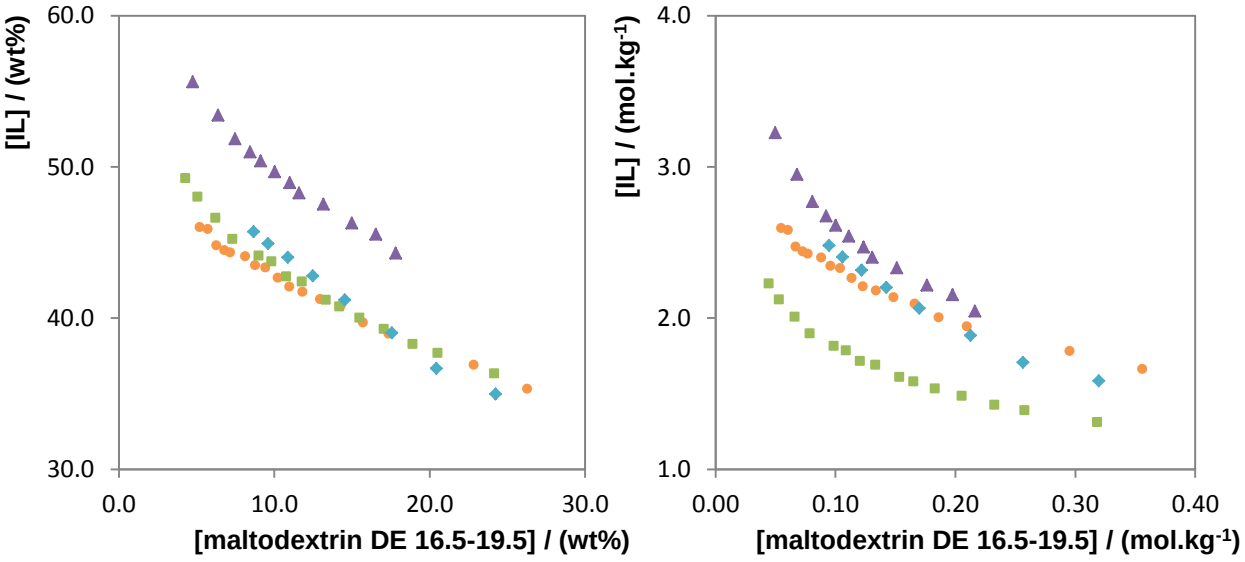

Figure 20. Phase diagrams for ternary systems composed of IL + maltodextrin DE 16.5-19.5 + H_2O at 298 K: ▲, $[P_{i(444)1}][Tos]$; ●, $[P_{4441}][MeSO_4]$; ■, $[P_{444(14)}]Cl$; ◆, $[P_{4444}]Br$ (left: wt%; right: mol.kg^{-1}).

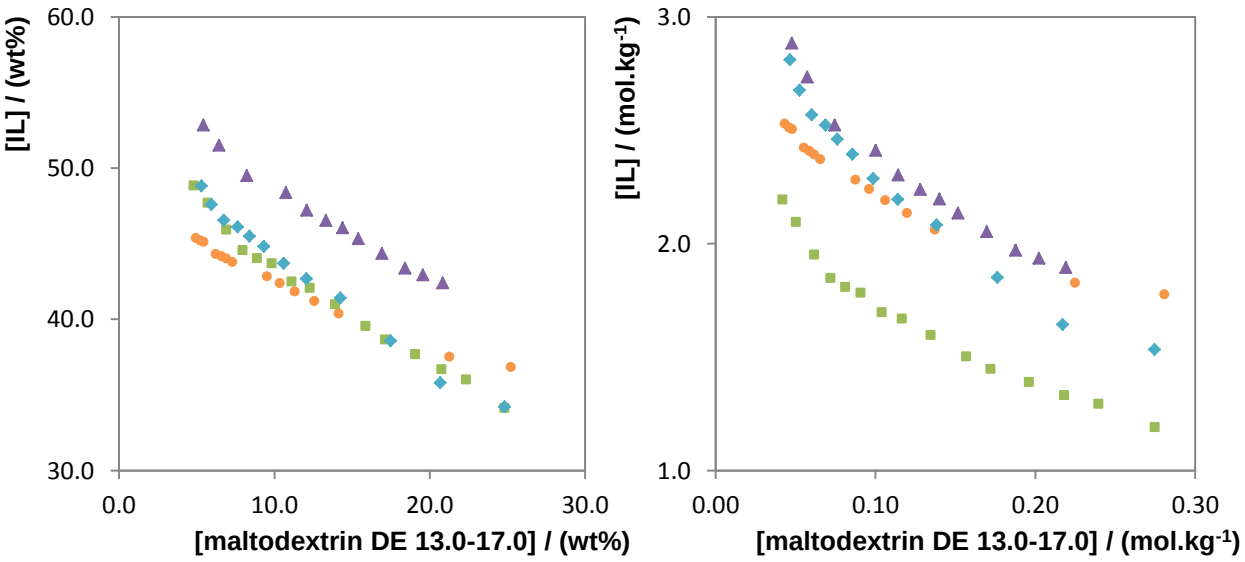

Figure 21. Phase diagrams for ternary systems composed of IL + maltodextrin DE 13.0-17.0 + H_2O at 298 K: ▲, $[P_{i(444)1}][Tos]$; ●, $[P_{4441}][MeSO_4]$; ■, $[P_{444(14)}]Cl$; ◆, $[P_{4444}]Br$ (left: wt%; right: mol.kg^{-1}).

The hydrophobicity and/or size of the cation shows a relevant role in ABS forming since amongst the studied ILs, $[P_{444(14)}]Cl$ is the most efficient IL for the

two-phase formation. On the other hand, the anion nature emerges now as less relevant for ABS splitting since $[P_{i(444)1}][Tos]$ is now the less effective IL for the creation of ABS with maltodextrins.

As mentioned before, the dextrose equivalent value is the most common parameter used to characterize the molecular weight of maltodextrins. In order to ascertain on the effect of the maltodextrin DE and/or the molecular weight variation on the formation of ABS systems, Figures 22 to 25 compares the obtained binodal curves for each IL with the two maltodextrin tested. It should be noted that maltodextrin DE 13.0-17.0 has a higher average molecular weight than maltodextrin DE 16.5-19.5, although the difference is not very large.

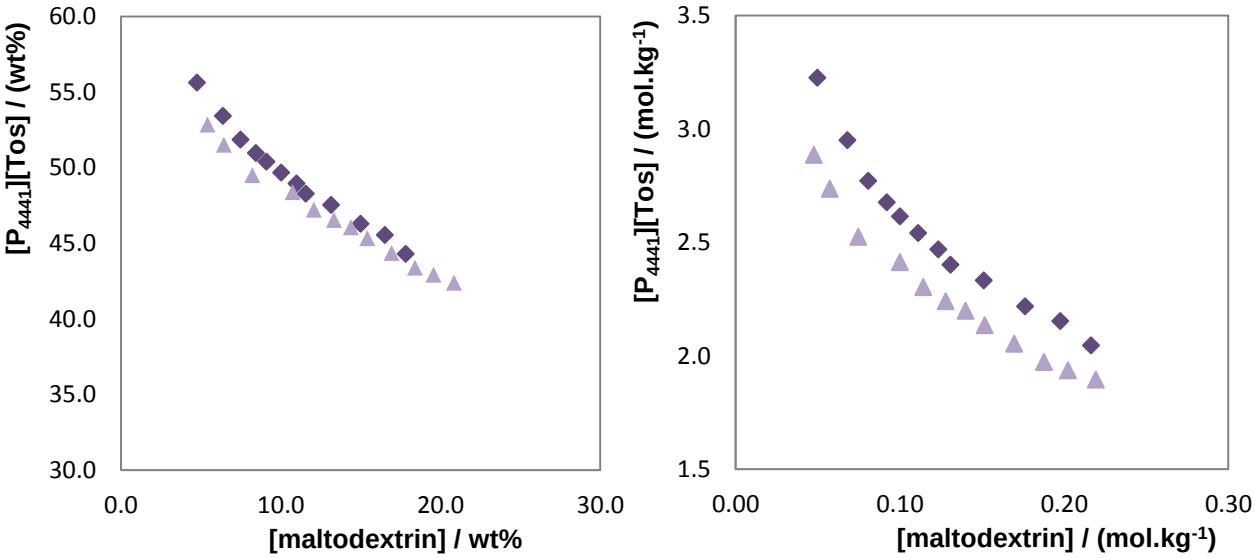

Figure 22. Phase diagrams for ternary systems composed of $[P_{i(444)1}][Tos]$ + maltodextrin + H_2O at 298 K: ◆, maltodextrin DE 16.5-19.5; ▲, maltodextrin DE 13.0-17.0 (left: wt%; right: $mol.kg^{-1}$).

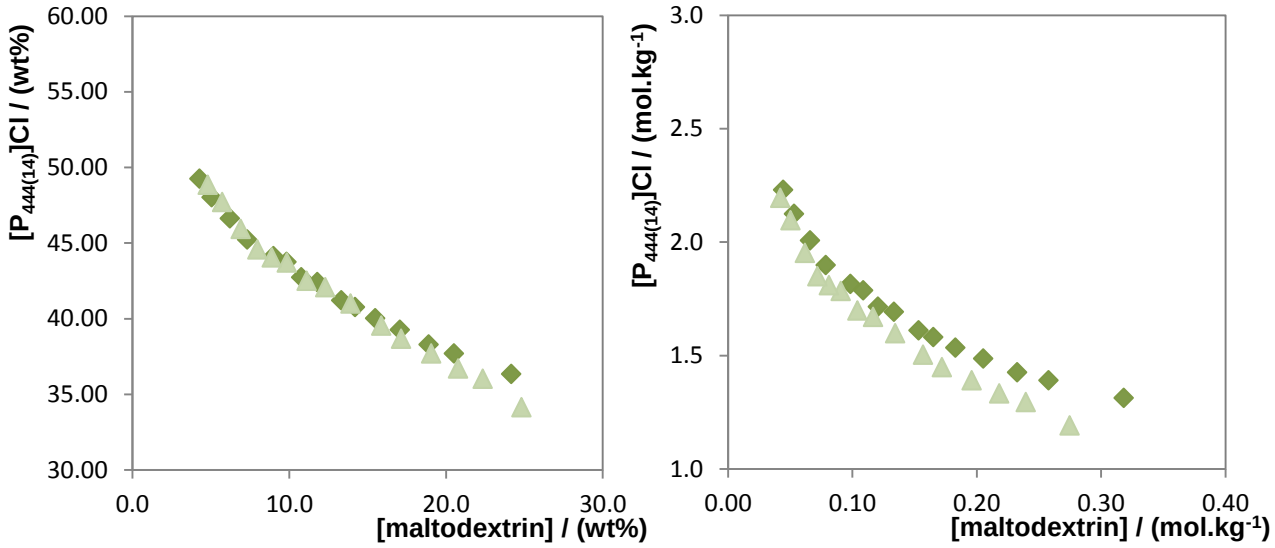

Figure 23. Phase diagrams for ternary systems composed of $[P_{444(14)}]Cl$ + maltodextrin + H_2O at 298 K: ◆, maltodextrin DE 16.5-19.5; ▲, maltodextrin DE 13.0-17.0 (left: wt%; right: mol.kg^{-1}).

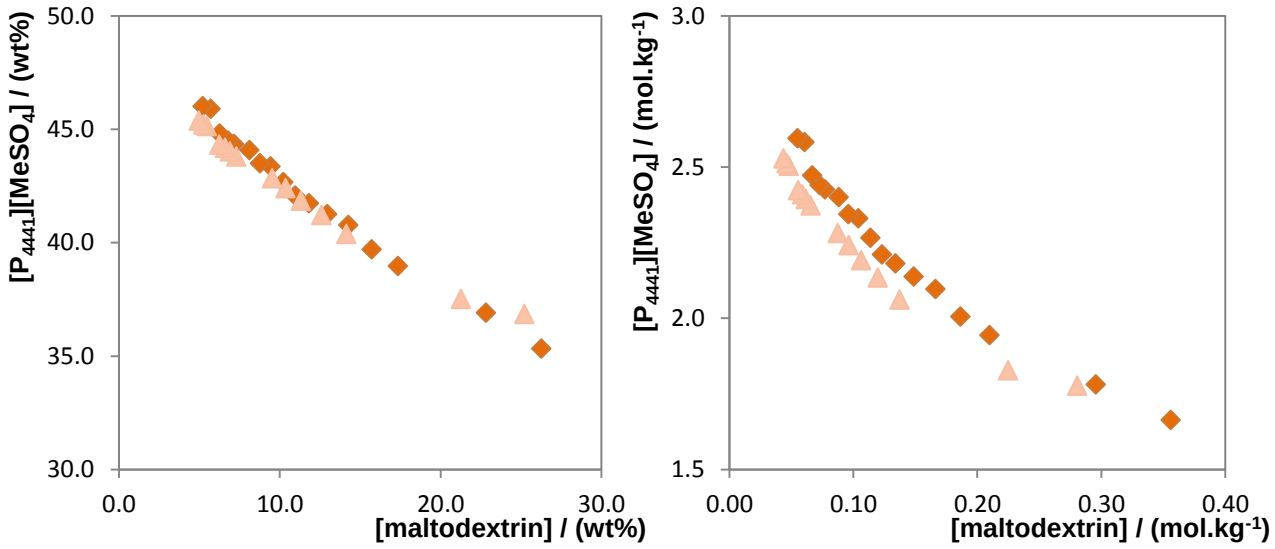

Figure 24. Phase diagrams for ternary systems composed of $[P_{4441}][MeSO_4]$ + maltodextrin + H_2O at 298 K: ◆, maltodextrin DE 16.5-19.5; ▲, maltodextrin DE 13.0-17.0 (left: wt%; right: mol.kg^{-1}).

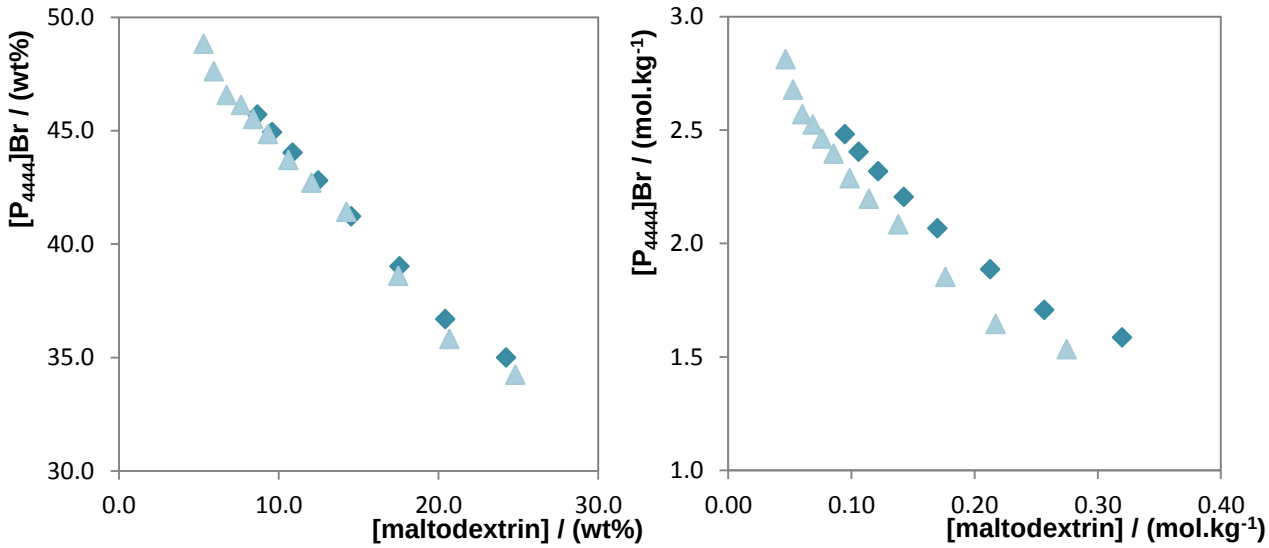

Figure 25. Phase diagrams for ternary systems composed of $[P_{4444}]Br$ + maltodextrin + H_2O at 298 K: ◆, maltodextrin DE 16.5-19.5; ▲, maltodextrin DE 13.0-17.0 (left: wt%; right: $mol.kg^{-1}$).

From the depicted results, it can be seen that both maltodextrins undergo phase separation at approximately the same extent. Since the difference between the two maltodextrin DE values (13.0-17.0 and 16.5-19.5) is not large, the obtained phase diagrams led to an overlapping, revealing identical solubilization and hydration behaviors. Nevertheless, it should be remarked that in molality units, maltodextrin DE 13.0-17.0 is more able to form ABS.

The experimental binodal data were again adjusted using the approach described by Merchuk et al.[29] through the empirical correlation described by Equation 1. For each ternary system, the regression parameters (*A*, *B* and *C*) and the respective standard deviation and correlation coefficient are reported in Table 4.

Table 4. Adjusted parameters used to describe the experimental binodal data for the phosphonium-based ILs + H_2O + maltodextrin systems by Equation 1.

IL + Maltodextrin + H_2O	*A*	*B*	*C*	R^2	100 sd [a]
[$P_{i(444)1}$][Tos]					
Maltodextrin DE 16.5-19.5	71.1001	-0.1142	-0.2865	0.9964	0.9956
Maltodextrin DE 13.0-17.0	64.9233	-0.0905	0.1656	0.9957	0.9948
[P_{4441}][MeSO4]					
Maltodextrin DE 16.5-19.5	55.1822	-0.0801	0.1900	0.9960	0.9954
Maltodextrin DE 13.0-17.0	53.4554	-0.0733	0.0606	0.9961	0.9953
[$P_{444(14)}$]Cl					
Maltodextrin DE 16.5-19.5	61.5976	-0.1110	-0.1322	0.9981	0.9978
Maltodextrin DE 13.0-17.0	61.5208	-0.1088	0.2499	0.9956	0.9948
[P_{4444}]Br					
Maltodextrin DE 16.5-19.5	64.8683	-0.1172	0.3290	0.9967	0,9954
Maltodextrin DE 13.0-17.0	61.9785	-0.1059	0.5120	0.9942	0.9930

[a] $sd = \left(\sum_{i=1}^{n} \left(w_{IL}^{cal} - w_{IL}^{exp} \right)^2 / n \right)^{0.5}$, where w_{IL}^{exp} is the experimental weight fraction of IL (described in Appendix A), w_{IL}^{cal} is the corresponding data calculated using Equation 1 and n represents the number of binodal data points.

4 Imidazolium-based ILs + H_2O + maltodextrin

4.1 Introduction

As shown before, maltodextrin is a promising salting-out inductor in the presence of ILs, and may embody an alternative route towards green and efficient biphasic systems to be used in industrial separation processes. In the previous section, phosphonium-based ILs as ABS promoters were evaluated. In this section, they were replaced by imidazolium-based ILs in order to ascertain on their feasibility and versatility.

Most of literature reports in literature describing ABS composed of ILs comprise the imidazolium-based family[8]. However, this work is the first evidence that imidazolium-based ILs are also able to form ABS with maltodextrin aqueous solutions. The unique properties of the imidazolium aromatic core can also be directly compared with the previous systems making use of tetralkylphosphonium-based compounds.

The chemical structure of ILs determines the intramolecular and intermolecular interactions and therefore their physicochemical properties. These properties can be finely tuned by varying the N-alkylimidazolium substituents or the constituting anion. Six imidazolium-based ILs were selected to infer on the cation side alkyl chain length and anion nature effects through their ternary phase diagrams with maltodextrin and water.

4.2 Experimental Section

4.2.1 Materials

The following ILs were tested: 1-butyl-3-methyl-imidazolium trifluoromethanesulfonate, [C_4mim][CF_3SO_3]; 1-butyl-3-methylimidazolium dicyanamide, [C_4mim][$N(CN)_2$]; 1-butyl-3-methylimidazolium ethylsulfate, [C_4mim][$EtSO_4$]; 1-butyl-3-methylimidazolium methylsulfate, [C_4mim][$MeSO_4$]; 1-butyl-3-methylimidazolium tetrafluoroborate, [C_4mim][BF_4]; 1-butyl-3-methylimidazolium thiocyanate, [C_4mim][SCN], 1-Butyl-3-methylimidazolium tosylate, [C_4mim][Tos] and 1-ethyl-3-methylimidazolium trifluoromethanesulfonate, [C_2mim][CF_3SO_3]. These ILs were supplied by Iolitec with a purity level > 98 wt %. The chemical structures of the studied ILs are presented in Figure 26. The purity of each IL was validated by ^{1}H, ^{13}C and ^{19}F NMR assays. Two maltodextrins of different DE value were tested: 13.0-17.0 and 16.5-19.5, both supplied by Aldrich.

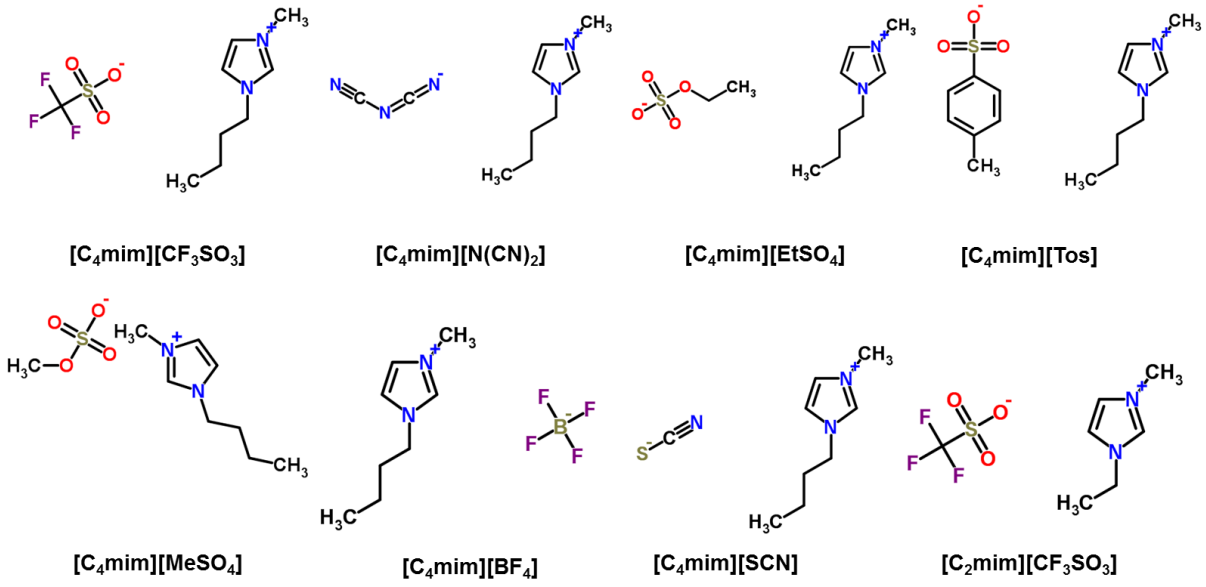

Figure 26. Chemical structure of the studied ILs: [C_4mim][CF_3SO_3]; [C_4mim][$N(CN)_2$]; [C_4mim][$EtSO_4$]; [C_4mim][Tos]; [C_4mim][$MeSO_4$]; [C_4mim][BF_4]; [C_4mim][SCN] and [C_2mim][CF_3SO_3].

4.2.2 Experimental Procedure

4.2.2.1 Phase Diagrams and Tie-Lines

Novel phase diagrams for imidazolium-based ILs + maltodextrin + water were determined in this work at 298 K. Aqueous solutions of maltodextrin (13.0-17.0 and 16.5-19.5) were prepared at 40 wt % combined with pure ILs or IL aqueous solutions at 80-90 wt %.

The binodal curves were determined at room temperature (298 ± 1) K and at atmospheric pressure through the cloud point titration method, as described in Section 3.2.2. The experimental binodal data were also fitted through the empiric correlation described by Equation 1.

The TLs were determined using prepared solutions with rigorous concentrations chosen from the biphasic region, where the amount of each component at the coexisting phases was determined. The prepared solutions were vigorously stirred on vortex (VWR™ International Vortex, VV3), and then centrifuged (Thermo Scientific, HERAEUS Megafure 16R) for 1 h at 3500 rpm and at controlled temperature (298 ± 1 K). Through this process the system undergoes the equilibrium by the separation into two different phases, which were carefully separated and weighted. Top and bottom phase components were quantified by a similar procedure described in Section 2.2.1.

Each TL was obtained by a quantitative analysis of the exact concentration of each compound on both phases. Both the top and bottom phases were analyzed. Maltodextrin was quantified by dry weight. Both phases were separated and to each one (*circa* 1 g) it was added ethanol (w:w = 1:2) to precipitate the maltodextrin. The samples were vortexed and then centrifuged at 3500 rpm and 298 K for 30 min. The ethanol upper liquid phase was then removed and maltodextrin was further twice washed with ethanol at the same proportions. Ethanol was finally evaporated in an air oven at constant temperature (± 333 K) for at least 48 h. The amount of maltodextrin at each phase was determined gravimetrically until constant weight. This procedure was previously optimized with known amounts of maltodextrin (circa 0.80 g) in aqueous solution (circa to 1.20 g of water) with recovery efficiencies in the order of (85 ± 1)% (result of 4 individual

vials with each maltodextrin). The water content in each phase was determined by evaporation until constant weight of dried IL + maltodextrin in an air oven at constant temperature (± 333 K) and for at least 48 h. The ILs amount was finally quantified by weight difference. Each sample was analyzed in duplicated vials to ascertain on the associated deviation.

4.3 Results and Discussion

Although there are several reports in the literature describing ABS comprising imidazolium-based ILs[8], this work is the first evidence that these hydrophilic ILs are also able to form ABS with maltodextrin aqueous solutions. The respective ternary phase diagrams, TLs and TLLs were determined here and are presented below.

4.3.1 Phase Diagrams and Tie-Lines

Two maltodextrins of different dextrose equivalents were tested (13.0-17.0 and 16.5-19.5 DE). Albeit several ILs have been tested, not all present ability to create ABS. Only $[C_4mim][CF_3SO_3]$, $[C_2mim][CF_3SO_3]$, $[C_4mim][EtSO_4]$, $[C_4mim][SCN]$ and $[C_4mim][BF_4]$ are able to form ABS with the studied maltodextrins. It was not detected the formation of ABS with $[C_4mim][MeSO_4]$, $[C_4mim][Tos]$ or $[C_4mim][N(CN)_2]$ independently of the maltodextrin dextrose equivalent. Figures 27 and 28 display the binodal curves for the systems that shown to undergo phase separation, divided into two sets according to the different maltodextrins used. In the absence of the molecular weight for maltodextrin, diagrams are presented in molality units or weight fraction for the IL concentration and in weight fraction for the maltodextrin. The corresponding and detailed binodal weight fraction data are presented in Appendix A.

The obtained results reveal that the ability of ILs for the formation ABS follows the same order for both maltodextrins: $[C_4mim][BF_4]$ > $[C_4mim][CF_3SO_3]$ > $[C_2mim][CF_3SO_3]$ > $[C_4mim][EtSO_4]$ > $[C_4mim][SCN]$. Since the cation is the same,

except in $[C_2mim][CF_3SO_3]$, this order reflects the decreasing hydrophobicity of the anion that enhances the IL hydration and hinders it salting-out by maltodextrin.

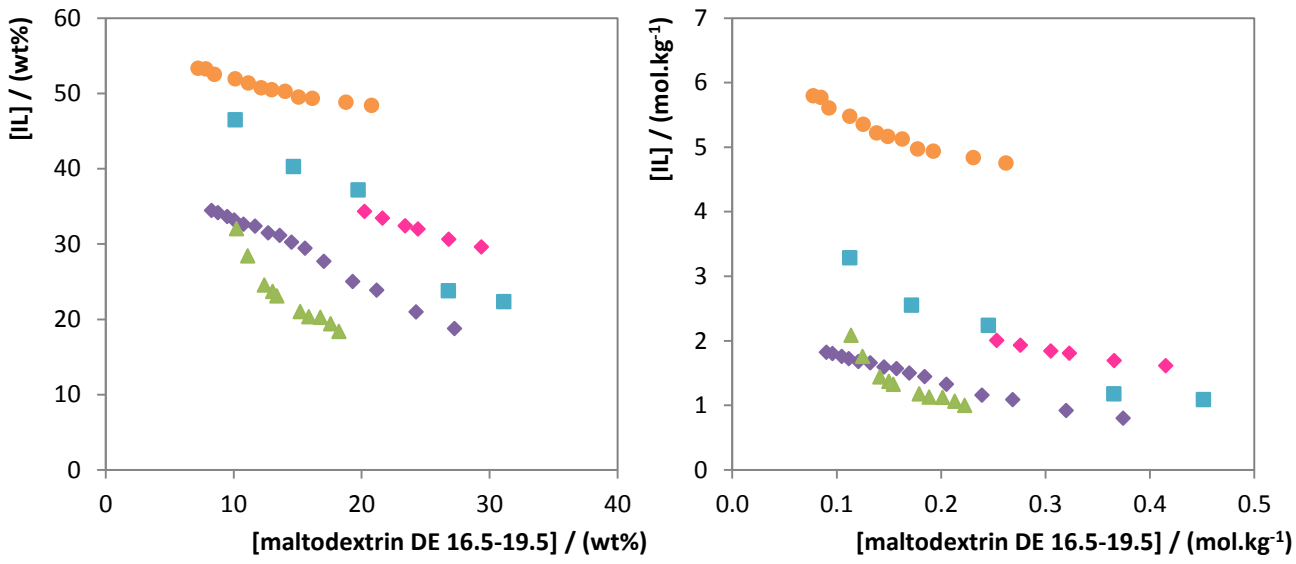

Figure 27. Phase diagrams for ternary systems composed of IL + maltodextrin DE 16.5-19.5 + H_2O at 298 K: ▲, $[C_4mim][BF_4]$; ◆, $[C_4mim][CF_3SO_3]$; ◆, $[C_2mim][CF_3SO_3]$; ■, $[C_4mim][EtSO_4]$; ●, $[C_4mim][SCN]$ (left: wt%; right: mol.kg^{-1}).

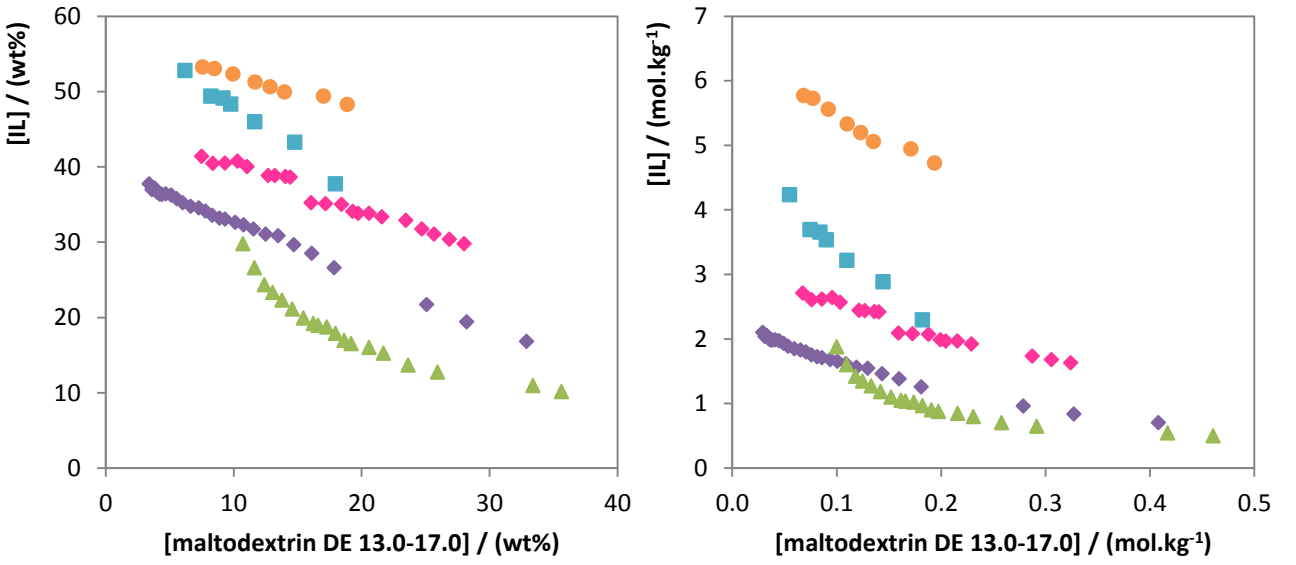

Figure 28. Phase diagrams for ternary systems composed of IL + maltodextrin DE 13.0-17.0 + H_2O at 298 K: ▲, $[C_4mim][BF_4]$; ◆, $[C_4mim][CF_3SO_3]$; ◆, $[C_2mim][CF_3SO_3]$; ■, $[C_4mim][EtSO_4]$; ●, $[C_4mim][SCN]$ (left: wt%; right: mol.kg^{-1}).

As previously noted, the DE value of maltodextrin is inversely proportional to the average molecular weight[95]. In order to ascertain on the effect of the

maltodextrin DE and/or the molecular weight variation through the formation of ABS, Figure 29 to 33 present the obtained binodal curves for each imidazolium-based IL with the two maltodextrins tested.

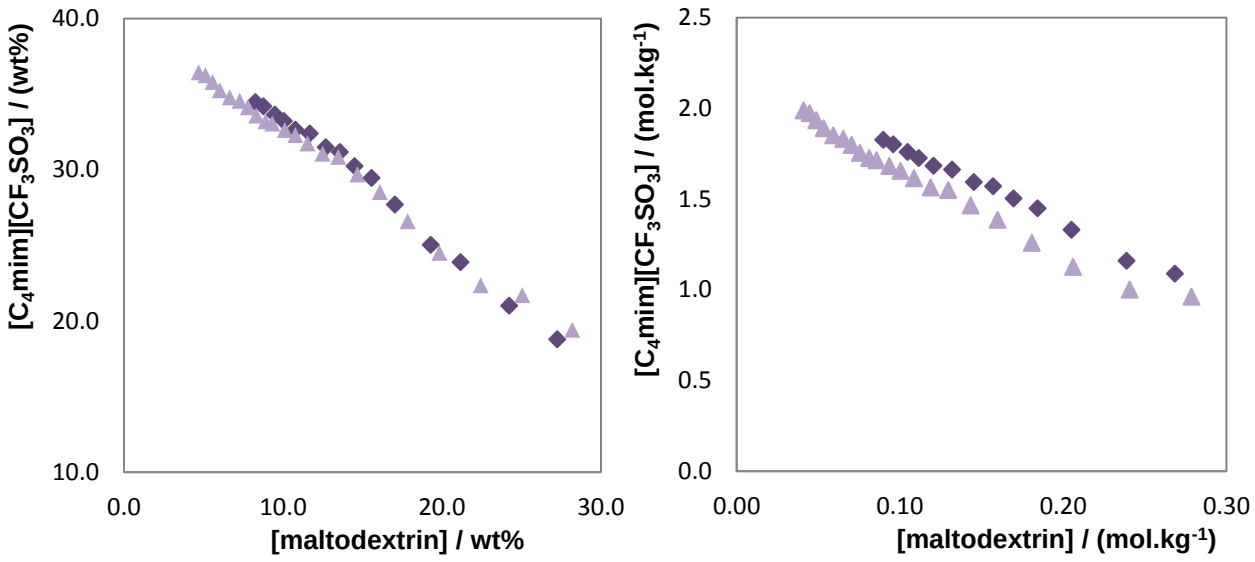

Figure 29. Phase diagrams for ternary systems composed of $[C_4mim][CF_3SO_3]$ + maltodextrin + H_2O at 298 K: ◆, maltodextrin DE 16.5-19.5; ▲, maltodextrin DE 13.0-17.0 (left: wt%; right: mol.kg^{-1}).

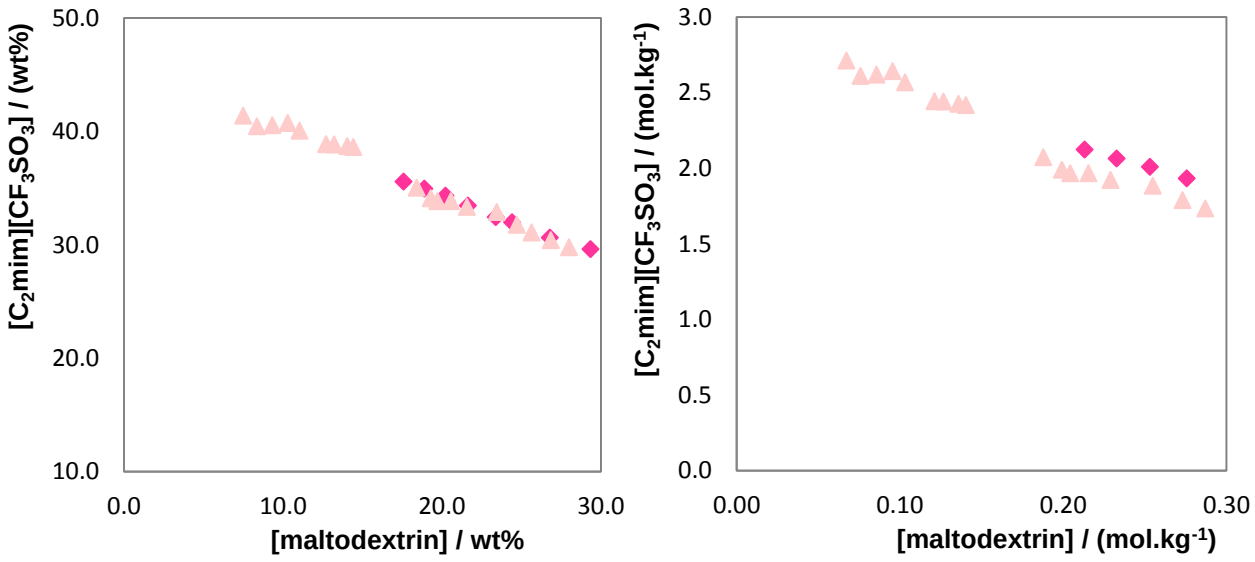

Figure 30. Phase diagrams for ternary systems composed of $[C_2mim][CF_3SO_3]$ + maltodextrin + H_2O at 298 K: ◆, maltodextrin DE 16.5-19.5; ▲, maltodextrin DE 13.0-17.0 (left: wt %; right: mol.kg^{-1}).

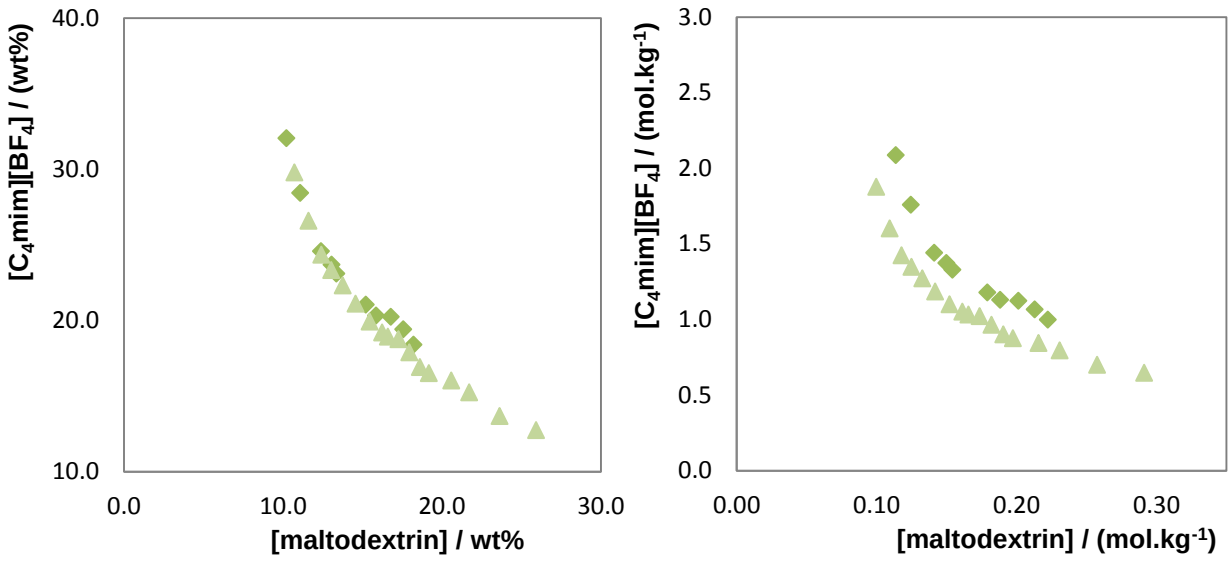

Figure 31. Phase diagrams for ternary systems composed of $[C_2mim][CF_3SO_3]$ + maltodextrin + H_2O at 298 K: ◆, maltodextrin DE 16.5-19.5; ▲, maltodextrin DE 13.0-17.0 (left: wt %; right: mol.kg^{-1}).

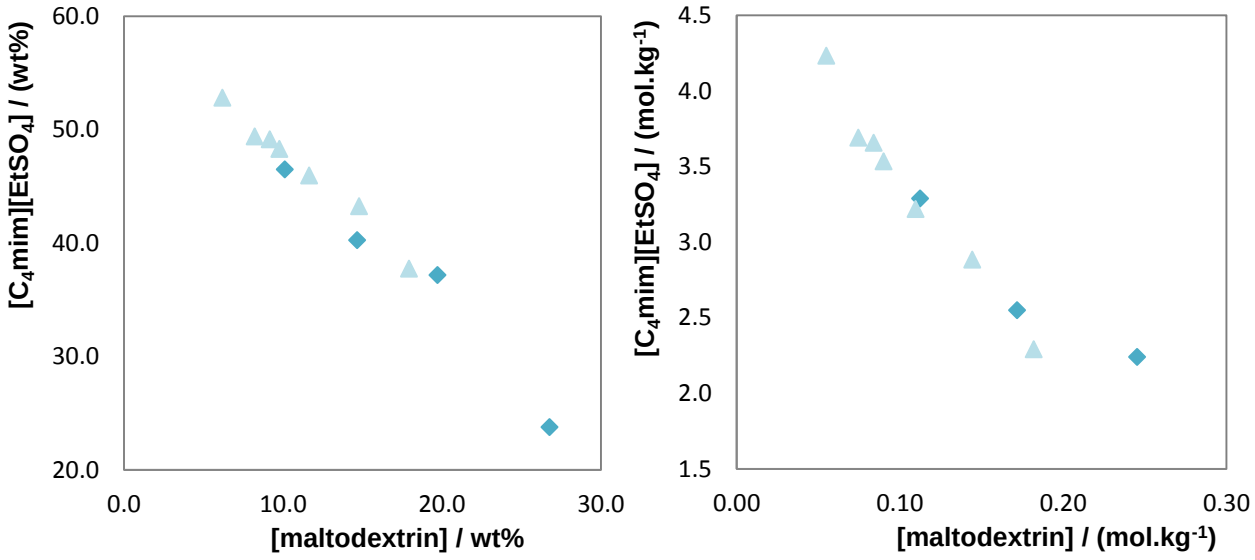

Figure 32. Phase diagrams for ternary systems composed of $[C_2mim][CF_3SO_3]$ + maltodextrin + H_2O at 298 K: ◆, maltodextrin DE 16.5-19.5; ▲, maltodextrin DE 13.0-17.0 (left: wt %; right: mol.kg^{-1}).

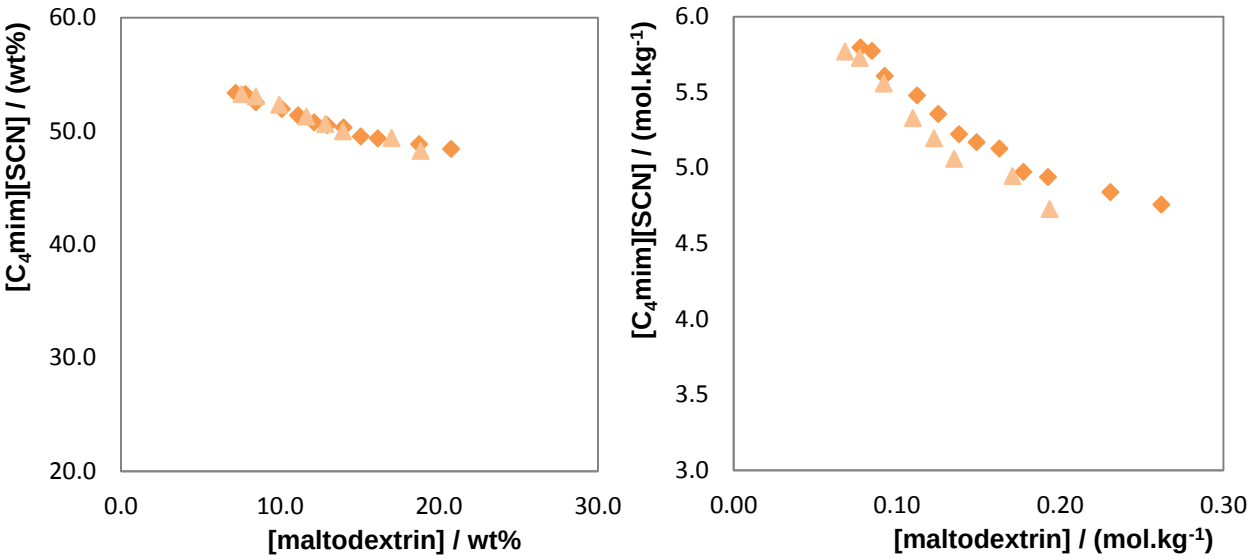

Figure 33. Phase diagrams for ternary systems composed of $[C_2mim][CF_3SO_3]$ + maltodextrin + H_2O at 298 K: ◆, maltodextrin DE 16.5-19.5; ▲, maltodextrin DE 13.0-17.0 (left: wt %; right: mol.kg^{-1}).

As previously observed with the phosphonium-based ILs, there are no large differences in the saturations curves as a function of the maltodextrin molecular weight.

The experimental binodal data were fitted using Equation 1. For each ternary system evaluated, the regression parameters *A*, *B* and *C*, and the respective standard deviation and correlation coefficient are reported in Table 5.

As an example, Figure 34 evidences the empirical correlation of the experimental data for the system composed of $[C_4mim][BF_4]$ + maltodextrin DE 13.0-17.0 + H_2O by Equation 1. The compositions of the ternary systems at equilibrium were determined as described in section 3.2.2. An example of the TLs obtained is also shown in Figure 34 for the same ternary system.

Table 5. Adjusted parameters used to describe the experimental binodal data for the imidazolium-based ILs + H_2O + maltodextrin systems by Equation 1.

IL + Maltodextrin + H_2O	*A*	*B*	10^5 *C*	R^2	100 sd [a]
[C_4mim][CF_3SO3]					
Maltodextrin DE 16.5-19.5	47.2598	-0.1038	2.0315	0.9945	0.9935
Maltodextrin DE 13.0-17.0	47.5765	-0.1178	1.1917	0.9905	0.9896
[C_2mim][CF_3SO3]					
Maltodextrin DE 16.5-19.5	60.2635	-0.1225	0.1990	0.9979	0.9970
Maltodextrin DE 13.0-17.0	52.2835	-0.0806	0.6687	0.9811	0.9787
[C_4mim][BF_4]					
Maltodextrin DE 16.5-19.5	74.1192	-0.3030	-0.1510	0.8411	0.8199
Maltodextrin DE 13.0-17.0	87.9441	-0.3687	0.0490	0.9932	0.9924
[C_4mim][C_2SO4]					
Maltodextrin DE 16.5-19.5	72.4556	-0.1346	1.6308	0.9696	0.9393
Maltodextrin DE 13.0-17.0	66.7912	-0.0952	2.7339	0.9888	0.9833
[C_4mim][SCN]					
Maltodextrin DE 16.5-19.5	64.3377	-0.0694	-0.3537	0.9935	0.9920
Maltodextrin DE 13.0-17.0	63.5249	-0.0630	-0.0190	0.9854	0.9796

[a] $sd = \left(\sum_{i=1}^{n} \left(w_{IL}^{cal} - w_{IL}^{exp} \right)^2 / n \right)^{0.5}$, where w_{IL}^{exp} is the experimental weight fraction of IL (described in Appendix A), w_{IL}^{cal} is the corresponding data calculated using Equation 1 and n represents the number of binodal data points.

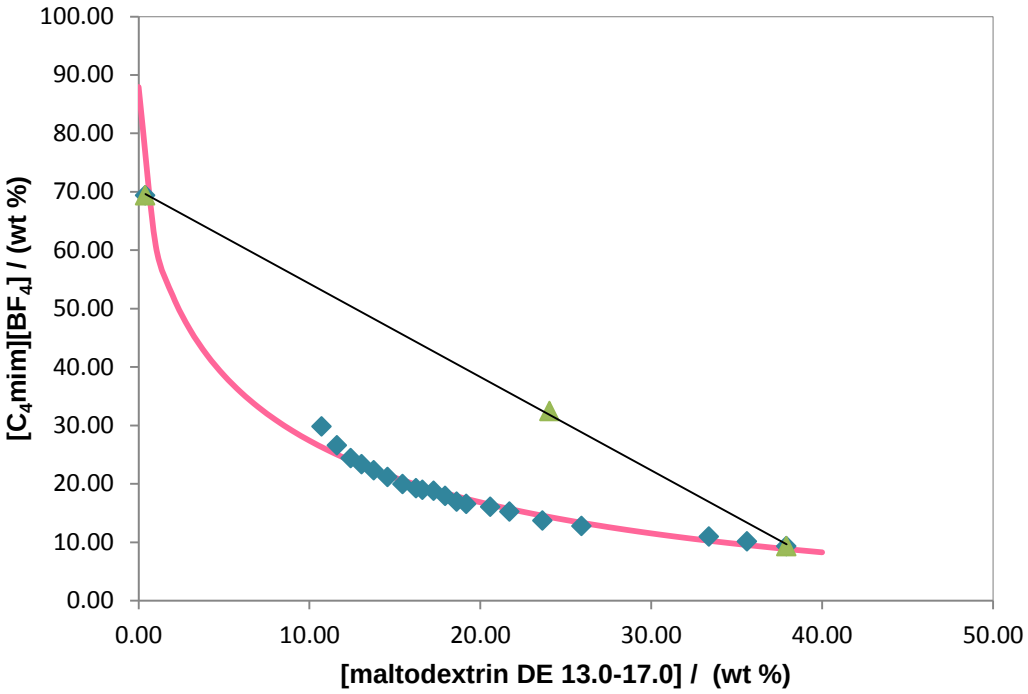

Figure 34. Phase diagrams for the $[C_4mim][BF_4]$ + maltodextrin DE 13.0-17.0 + H_2O ternary system at 298 K: ◆, Experimental data; —, fitting by eq.1; ▲, TL 1.

Finally, a general comparison on the ability of the different polysaccharides studied to form ABS with ILs can be made based on the previous experimental data. Figure 35 shows the direct comparison between dextran and maltodextrin to form ABS with a common IL. On the other hand, Figure 36 compares the imidazolium *versus* phosphonium ILs ability to form ABS with a common polysaccharide.

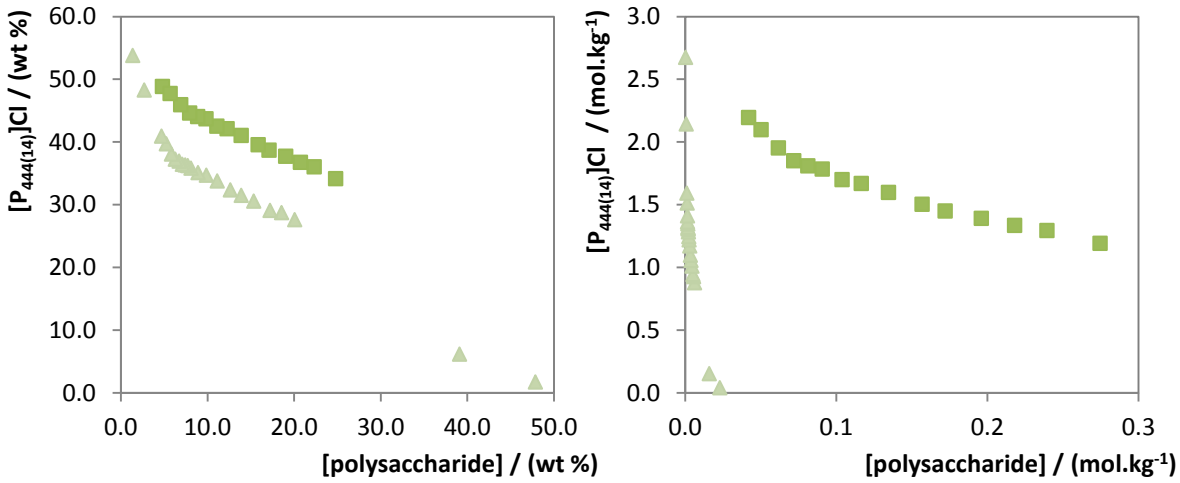

Figure 35. Phase diagrams for ternary systems composed of $[P_{444(14)}]Cl$ + polysaccharide + H_2O at 298 K: ■, maltodextrin DE 13.0-17.0; ▲, dextran 40 kDa.

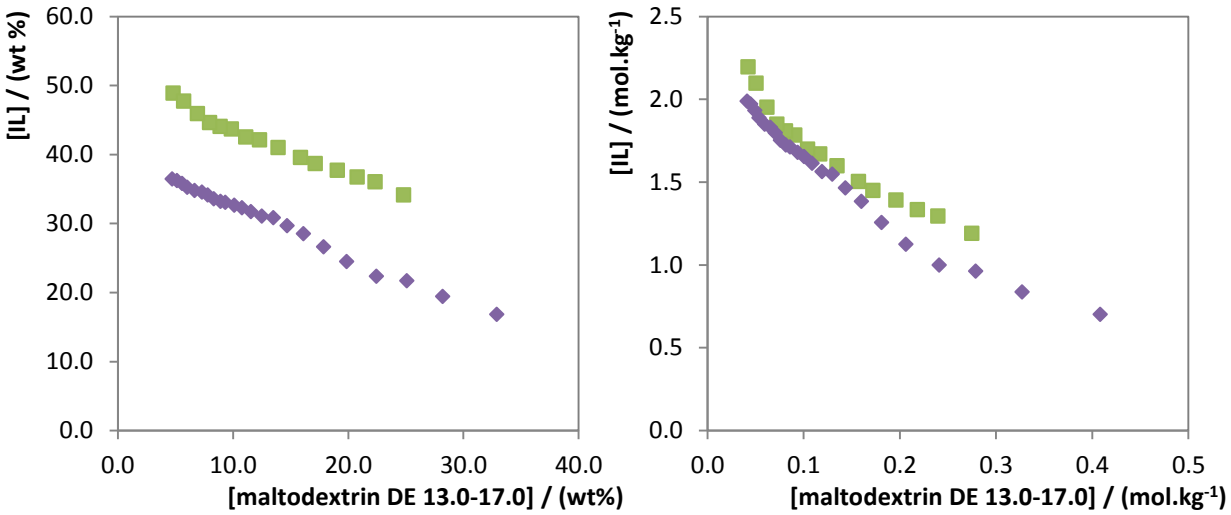

Figure 36. Phase diagrams for ternary systems composed of IL + maltodextrin DE 13.0-17.0 + H_2O at 298 K: ■, $[P_{444(14)}]Cl$; ◆, $[C_4mim][CF_3SO_3]$.

In general, dextran enables an easier ABS formation than maltodextrin when in the presence of a common IL, what could be explained by the intrinsic characteristics of each polysaccharide. As previously seen in Figure 7, both of them are composed of glucose monomers, yet with different properties. Maltodextrin is mainly formed by linear chains of monomers whereas dextran links each monomer by 1-6 or 1-3 linkages, leading to numerous chain-branches

through its structure. This phenomenon can lead to a different capability for solute-solvent interactions so that solubility decreases with branching.

On the other hand, and for the same carbohydrate, the results reveal that imidazolium-based ILs composed of a fluorinate anion are more easily excluded to a second liquid phase in the presence of maltodextrin in aqueous media when compared with phosphonium-based ILs. However, it should be highlighted that it would be interesting to test phosphonium-based ILs composed of fluorinated anions and their ABS formation ability.

A closer look at the phase diagrams shown reveals a slight inflection in the curves for the compositions with variable weight of polysaccharide (10-25 %). The inflection point depends on the carbohydrate molecular identity, but also on the IL, as Figures 35 and 36 evidence. The inflection seems nearly coincidental for both maltodextrin types, and at least partially independent of their molecular weight, but that may result from the small DE value difference. This seems to be corroborated by Figure 35, where both natural polysaccharides are compared. These data clearly establish the necessity of a deeper investigation to address the two phase formation process and in particular to unveil the influence of the natural polymer characteristics in the two-phase formation mechanism.

5 Final Remarks

5.1 Conclusions

With the intent of finding more benign and sustainable approaches, for the first time it was addressed the evaluation and characterization of several ABS composed of IL + polysaccharides + H_2O. IL-polysaccharide-based aqueous biphasic systems appear as promising separation processes since they provide efficient extractions while maintaining a suitable aqueous environment for biomolecules.

In this work, it was intended to fill the gap in the study of phosphonium-based ILs and to introduce new polysaccharides to form ABS; two families of ILs, phosphonium- and imidazolium-based, and two polysaccharides of different molecular weight, dextran and maltodextrin, were investigated.

From the ABS studied that are composed of phosphonium-based ILs and dextran, $[P_{i(444)1}][Tos]$, $[P_{4441}][MeSO_4]$, $[P_{444(14)}]Cl$ and $[P_{4444}]Br$ are able to form ABS with the three dextrans investigated. However, it was not detected the formation of aqueous biphasic systems with $[P_{4444}]Cl$ or $[P_{4442}][Et_2PO_4]$ independently of the dextran molecular weight. The ability of ILs to form ABS follows the rank: $[P_{i(444)1}][Tos] > [P_{444(14)}]Cl > [P_{4444}]Br > [P_{4441}][MeSO_4]$. The same set of phosphonium ILs was appraised regarding their aptitude to form ABS with maltodextrins. Again, $[P_{4444}]Cl$ or $[P_{4442}][Et_2PO_4]$ are not able to form ABS with polysaccharides. In addition, for those that form ABS, their ability for phase-separation follows the order: $[P_{444(14)}]Cl > [P_{4441}][MeSO_4] > [P_{4444}]Br > [P_{i(444)1}][Tos]$.

Finally, imidazolium-based ILs were also investigated as phase-forming components of ABS with maltodexrtins. $[C_4mim][CF_3SO_3]$, $[C_2mim][CF_3SO_3]$, $[C_4mim][EtSO_4]$, $[C_4mim][SCN]$ and $[C_4mim][BF_4]$ were able to form two-phase systems with maltodextrins. On the other hand, it was not detected the formation of ABS with $[C_4mim][MeSO_4]$, $[C_4mim][Tos]$ or $[C_4mim][N(CN)_2]$. The obtained results reveal that the ability of ILs for the formation of ABS follows the same order for both maltodextrins: $[C_4mim][BF_4] > [C_4mim][CF_3SO_3] > [C_2mim][CF_3SO_3] > [C_4mim][EtSO_4] > [C_4mim][SCN]$.

In summary, for the same IL, dextran is more able to induce the ABS formation when compared with the other salting-out agent studied (maltodextrin). This could be partially explained by the hydroxyl content of each polysaccharide, but the contribution of other factors is certainly present. Furthermore, for the same carbohydrate, the results reveal that imidazolium-based ILs combined with fluorinated anions are greater ABS inductors when compared with phosphonium-based ILs.

5.2 Future Work

In view of the great interest in developing cost-effective, greener and eco-friendly separation techniques there is a high importance to continue the investigation started in this work. In particular, it would be interesting to infer on the molecular-level mechanisms or salting-out phenomenon responsible for the liquid-liquid demixing by the use of spectroscopic techniques.

Finally, and taking into account that these novel systems are more benign than most IL-based ABS reported to date, it would be valuable to investigate their extractive performance for a wide variety of biomolecules to screen their potential application.

6 References

1. U. NATIONS, Convention on Biological Diversity, http://www.cbd.int/, Accessed December/2012.

2. C. R. Cantor, *Trends in Biotechnology*, 2000, **18**, 6-7.

3. M. Gavrilescu and Y. Chisti, *Biotechnology Advances*, 2005, **23**, 471-499.

4. N. Lima, *Biotecnologia : fundamentos e aplicações*, Lidel, Lisboa, 2003.

5. P. L. Show, C. P. Tan, M. Shamsul Anuar, A. Ariff, Y. A. Yusof, S. K. Chen and T. C. Ling, *Bioresource Technology*, 2012, **116**, 226-233.

6. P.-Å. Albertsson, in *Advances in Protein Chemistry*, eds. J. T. E. C.B. Anfinsen and M. R. Frederic, Academic Press, 1970, vol. Volume 24, pp. 309-341.

7. S. P. M. Ventura, R. L. F. de Barros, J. M. de Pinho Barbosa, C. M. F. Soares, A. S. Lima and J. A. P. Coutinho, *Green Chemistry*, 2012, **14**, 734-740.

8. M. G. Freire, A. F. M. Claudio, J. M. M. Araujo, J. A. P. Coutinho, I. M. Marrucho, J. N. C. Lopes and L. P. N. Rebelo, *Chemical Society Reviews*, 2012, **41**, 4966-4995.

9. M. G. Freire, J. F. Pereira, M. Francisco, H. Rodríguez, L. P. Rebelo, R. D. Rogers and J. A. Coutinho, *Chemistry*, 2012, **18**, 1831-1839.

10. F. Ruiz-Ruiz, J. Benavides, O. Aguilar and M. Rito-Palomares, *Journal of Chromatography A*, 2012, **1244**, 1-13.

11. H. Passos, A. R. Ferreira, A. F. M. Cláudio, J. A. P. Coutinho and M. G. Freire, *Biochemical Engineering Journal*, 2012, **67**, 68-76.

12. K. E. Gutowski, G. A. Broker, H. D. Willauer, J. G. Huddleston, R. P. Swatloski, J. D. Holbrey and R. D. Rogers, *Journal of the American Chemical Society*, 2003, **125**, 6632-6633.

13. S. Keskin, D. Kayrak-Talay, U. Akman and Ö. Hortaçsu, *The Journal of Supercritical Fluids*, 2007, **43**, 150-180.

14. T. Welton, *Chemical Reviews*, 1999, **99**, 2071-2084.

15. C. Lagrost, D. Carrie, M. Vaultier and P. Hapiot, *Journal of Physical Chemistry a*, 2003, **107**, 745-752.

16. T. P. Thuy Pham, C.-W. Cho and Y.-S. Yun, *Water Research*, 2010, **44**, 352-372.

17. C. M. S. S. Neves, S. n. P. M. Ventura, M. G. Freire, I. M. Marrucho and J. o. A. P. Coutinho, *The Journal of Physical Chemistry B*, 2009, **113**, 5194-5199.

18. L. M. N. B. F. Santos, J. N. Canongia Lopes, J. A. P. Coutinho, J. M. S. S. Esperança, L. R. Gomes, I. M. Marrucho and L. P. N. Rebelo, *Journal of the American Chemical Society*, 2006, **129**, 284-285.

19. R. Sedev, *Current Opinion in Colloid & Interface Science*, 2011, **16**, 310-316.

20. T. Welton, *Coordination Chemistry Reviews*, 2004, **248**, 2459-2477.

21. P. Kubisa, *Progress in Polymer Science*, 2009, **34**, 1333-1347.

22. M. Moniruzzaman, K. Nakashima, N. Kamiya and M. Goto, *Biochemical Engineering Journal*, 2010, **48**, 295-314.

23. J. Hao and T. Zemb, *Current Opinion in Colloid & Interface Science*, 2007, **12**, 129-137.

24. Q. Cao, L. Quan, C. He, N. Li, K. Li and F. Liu, *Talanta*, 2008, **77**, 160-165.

25. Y. L. Li and M. L. Gross, *Journal of the American Society for Mass Spectrometry*, 2004, **15**, 1833-1837.

26. C.-Z. Liu, F. Wang, A. R. Stiles and C. Guo, *Applied Energy*, 2012, **92**, 406-414.

27. S. P. M. Ventura, C. S. Marques, A. A. Rosatella, C. A. M. Afonso, F. Gonçalves and J. A. P. Coutinho, *Ecotoxicology and Environmental Safety*, 2012, **76**, 162-168.

28. G. C. Kresheck and Z. Wang, *Journal of Chromatography B*, 2007, **858**, 247-253.

29. J. C. Merchuk, B. A. Andrews and J. A. Asenjo, *Journal of Chromatography B: Biomedical Sciences and Applications*, 1998, **711**, 285-293.

30. L. Bulgariu, D. Bulgariu, I. Sârghie and T. Măluțan, *Central European Journal of Chemistry*, 2007, **5**, 291-302.

31. Y. Akama, M. Ito and S. Tanaka, *Talanta*, 2000, **53**, 645-650.

32. P. Vázquez-Villegas, O. Aguilar and M. Rito-Palomares, *Separation and Purification Technology*, 2011, **78**, 69-75.

33. G. Yixin, M. Lehe and Z. Ziqiang, *Biotechnology Techniques*, 1994, **8**, 491-496.

34. C. Yu, J. Han, Y. Wang, Y. Yan, S. Hu, Y. Li and X. Zhao, *Thermochimica Acta*, 2011, **523**, 221-226.

35. J. F. B. Pereira, L. P. N. Rebelo, R. D. Rogers, J. A. P. Coutinho and M. G. Freire, *Physical Chemistry Chemical Physics*, 2013, **15**, 19580-19583.

36. J. G. Huddleston, A. E. Visser, W. M. Reichert, H. D. Willauer, G. A. Broker and R. D. Rogers, *Green Chemistry*, 2001, **3**, 156-164.

37. S. n. P. M. Ventura, C. M. S. S. Neves, M. G. Freire, I. M. Marrucho, J. o. Oliveira and J. o. A. P. Coutinho, *The Journal of Physical Chemistry B*, 2009, **113**, 9304-9310.

38. M. G. Freire, C. L. S. Louros, L. P. N. Rebelo and J. A. P. Coutinho, *Green Chemistry*, 2011, **13**, 1536-1545.

39. Y. Zhang, S. Zhang, Y. Chen and J. Zhang, *Fluid Phase Equilibria*, 2007, **257**, 173-176.

40. M. T. Zafarani-Moattar and S. Hamzehzadeh, *Journal of Chemical & Engineering Data*, 2010, **55**, 1598-1610.

41. Y. Chen, Y. Wang, Q. Cheng, X. Liu and S. Zhang, *The Journal of Chemical Thermodynamics*, 2009, **41**, 1056-1059.

42. C. Wu, J. Wang, Y. Pei, H. Wang and Z. Li, *Journal of Chemical & Engineering Data*, 2010, **55**, 5004-5008.

43. B. Wu, Y. M. Zhang and H. P. Wang, *Journal of Chemical & Engineering Data*, 2008, **53**, 983-985.

44. B. Nicolaus, L. Lama, A. Panico, V. S. Moriello, I. Romano and A. Gambacorta, *Systematic and Applied Microbiology*, 2002, **25**, 319-325.

45. D. Knorr, *Trends in Food Science & Technology*, 1998, **9**, 295-306.

46. I. W. Sutherland, *International Dairy Journal*, 2001, **11**, 663-674.

47. B. Nicolaus, M. Kambourova and E. T. Oner, *Environmental Technology*, 2010, **31**, 1145-1158.

48. A. Poli, G. Anzelmo and B. Nicolaus, *Marine Drugs*, 2010, **8**, 1779-1802.

49. K. Pavlova, S. Rusinova-Videva, M. Kuncheva, M. Kratchanova, M. Gocheva and S. Dimitrova, *Appl Biochem Biotechnol*, 2011, **163**, 1038-1052.

50. sigmaaldrich.com, http://www.sigmaaldrich.com/life-science/biochemicals/biochemical-products.html?TablePage=22696471, Accessed December/2012.

51. M. H. P. B. Vettori, R. Mukerjea and J. F. Robyt, *Carbohydrate Research*, 2011, **346**, 1077-1082.

52. A. N. de Belder, in *Ullmann's Encyclopedia of Industrial Chemistry*, Wiley-VCH Verlag GmbH & Co. KGaA, 2000.

53. E. C. SCIENTIFIC COMMITTEE ON FOOD, *HEALTH & CONSUMER PROTECTION DIRECTORATE-GENERAL*, 2000.

54. H. Neubauer, A. Bauché and B. Mollet, *Microbiology (Reading, England)*, 2003, **149**, 973-982.

55. I. L. EUl Qader SA, Aman A, Shireen E, Azhar A., *Turkish Journal of Biochemistry*, 2005, **31**, 21-26.

56. A. Aman, N. N. Siddiqui and S. A. U. Qader, *Carbohydrate Polymers*, 2012, **87**, 910-915.

57. G. A. Burdock and I. G. Carabin, *Toxicology Letters*, 2004, **150**, 3-18.

58. S. Ghosh, R. Vijayalakshmi and T. Swaminathan, *Biochemical Engineering Journal*, 2004, **21**, 241-252.

59. M. W. Kearsley and S. Z. Dziedzic, *Handbook of starch hydrolysis products and their derivatives*, Blackie Academic & Professional, London; New York, 1995.

60. L. M. Marchal, H. H. Beeftink and J. Tramper, *Trends in Food Science & Technology*, 1999, **10**, 345-355.

61. E. F. S. Authority, *The EFSA Journal*, 2007, 1-7.

62. J. Sun, R. Zhao, J. Zeng, G. Li and X. Li, *Molecules*, 2010, **15**, 5162-5173.

63. E. Storz and K.-J. Steffens, *Starch - Stärke*, 2004, **56**, 58-62.

64. Y. Chen and S. Zhang, *Journal of Chemical & Engineering Data*, 2009, **55**, 278-282.

65. B. Wu, Y. Zhang and H. Wang, *The Journal of Physical Chemistry B*, 2008, **112**, 6426-6429.

66. B. Wu, Y. Zhang, H. Wang and L. Yang, *The Journal of Physical Chemistry B*, 2008, **112**, 13163-13165.

67. Y. Chen, Y. Meng, S. Zhang, Y. Zhang, X. Liu and J. Yang, *Journal of Chemical & Engineering Data*, 2010, **55**, 3612-3616.

68. H. Olivier-Bourbigou, L. Magna and D. Morvan, *Applied Catalysis A: General*, 2010, **373**, 1-56.

69. Z. Breitbach and D. Armstrong, *Anal Bioanal Chem*, 2008, **390**, 1605-1617.

70. CYTEC, Phosphine Specialties, www.cytec.com/, Accessed December/2012.

71. E. Antoniou and M. Tsianou, *Journal of Applied Polymer Science*, 2012, **125**, 1681-1692.

72. T. Lütke-Eversloh, C. Santos and G. Stephanopoulos, *Appl Microbiol Biotechnol*, 2007, **77**, 751-762.

73. P. K. Pallaghy, A. P. Melnikova, E. C. Jimenez, B. M. Olivera and R. S. Norton, *Biochemistry*, 1999, **38**, 11553-11559.

74. H. D. Willauer, J. G. Huddleston and R. D. Rogers, *Industrial & Engineering Chemistry Research*, 2002, **41**, 1892-1904.

75. S. Carvalho, Final Report, University of Aveiro, 2012.

76. C. Reichardt, *Green Chemistry*, 2005, **7**, 339-351.

77. A. F. M. Cláudio, A. M. Ferreira, S. Shahriari, M. G. Freire and J. A. P. Coutinho, *The Journal of Physical Chemistry B*, 2011, **115**, 11145-11153.

78. L. Crowhurst, P. R. Mawdsley, J. M. Perez-Arlandis, P. A. Salter and T. Welton, *Physical Chemistry Chemical Physics*, 2003, **5**, 2790-2794.

79. A. Brandt, J. P. Hallett, D. J. Leak, R. J. Murphy and T. Welton, *Green Chemistry*, 2010, **12**, 672-679.

80. R. Lungwitz, V. Strehmel and S. Spange, *New Journal of Chemistry*, 2010, **34**, 1135-1140.

81. T. Mourão, A. F. M. Cláudio, I. Boal-Palheiros, M. G. Freire and J. A. P. Coutinho, *The Journal of Chemical Thermodynamics*, 2012, **54**, 398-405.

82. E. Antoniou, C. F. Buitrago, M. Tsianou and P. Alexandridis, *Carbohydrate Polymers*, 2010, **79**, 380-390.

83. C. E. Ioan, T. Aberle and W. Burchard, *Macromolecules*, 2000, **33**, 5730-5739.

84. T. D. Leathers, in *Biopolymers*, ed. S. D. B. Erick J. Vandamme, Alexander Steinbüchel, Wiley-VCH, Weinheim, 2002, vol. 5, pp. 229-321.

85. A. R. Shultz and P. J. Flory, *Journal of the American Chemical Society*, 1953, **75**, 5681-5685.

86. H. Mazi, B. Zümreoğlu-Karan and A. Güner, *Journal of Applied Polymer Science*, 2001, **82**, 323-329.

87. R. Mehvar, *Journal of Controlled Release*, 2000, **69**, 1-25.

88. C. L. S. Louros, A. F. M. Cláudio, C. M. S. S. Neves, M. G. Freire, I. M. Marrucho, J. Pauly and J. A. P. Coutinho, *International Journal of Molecular Sciences*, 2010, **11**, 1777-1791.

89. M. T. Zafarani-Moattar and S. Hamzehzadeh, *Biotechnology Progress*, 2011, **27**, 986-997.

90. M. T. Zafarani-Moattar, S. Hamzehzadeh and S. Nasiri, *Biotechnology Progress*, 2012, **28**, 146-156.

91. A. Salabat, M. H. Abnosi and A. Motahari, *Journal of Chemical & Engineering Data*, 2008, **53**, 2018-2021.

92. M. Lu and F. Tjerneld, *Journal of Chromatography A*, 1997, **766**, 99-108.

93. U. S. F. a. D. Administration, Revised as of April 1, 2013 edn., vol. Title 21, Volume 3.

94. C. Loret, V. Meunier, W. J. Frith and P. J. Fryer, *Carbohydrate Polymers*, 2004, **57**, 153-163.

95. Y. Rong, M. Sillick and C. M. Gregson, *Journal of Food Science*, 2009, **74**, C33-C40.

Appendix A

Experimental Binodal Data

The experimental weight fraction data for the phase diagrams of the systems composed of IL + Polysaccharide + H_2O are presented in Tables A1 to A7.

Table A 1. Experimental weight fraction data for the systems composed of dextran 6 kDa (1) + IL (2) + H_2O (3) at 298.15 K and atmospheric pressure.

[$P_{i(444)1}$][Tos]		**[$P_{444(14)}$]Cl**		**[P_{4444}]Br**	
***M_W* = 388.55**		***M_W* = 435.15**		***M_W* = 339.33**	
100 *w*1	**100 *w*2**	**100 *w*1**	**100 *w*2**	**100 *w*1**	**100 *w*2**
47.628	11.776	51.107	9.980	42.520	13.682
43.912	12.837	42.360	9.748	42.167	13.621
30.452	21.776	8.010	48.695	30.596	21.167
19.720	29.915	7.094	49.967	26.362	24.928
13.841	36.478	6.424	50.701	22.753	28.153
10.989	37.766	6.022	51.165	19.319	30.789
7.417	42.593	5.368	51.950	15.577	34.310
6.277	44.903	4.923	52.241	13.922	36.212
4.973	54.679	13.884	41.940	12.692	37.054
3.770	54.432	11.142	44.810	10.813	39.964
		8.622	47.417	9.562	40.912
		5.167	51.696	7.810	45.452
		4.319	53.058	6.338	45.976
		3.502	57.435	1.999	58.720
		2.496	66.091	1.494	58.971
[P_{4441}][$MeSO_4$]		**[P_{4441}][$MeSO_4$]**		**[P_{4441}][$MeSO_4$]**	
***M_W* = 328.45**		***M_W* = 328.45**		***M_W* = 328.45**	
100 *w*1	**100 *w*2**	**100 *w*1**	**100 *w*2**	**100 *w*1**	**100 *w*2**
29.092	26.818	10.917	39.027	44.972	13.457
26.116	27.816	10.381	39.622	39.976	15.879
23.028	29.811	9.739	40.127	7.507	44.584
20.185	32.769	9.221	40.627	6.289	43.240
18.422	33.578	8.813	41.181	5.857	44.060
16.368	35.021	8.458	41.435	5.317	44.605
15.192	35.861	8.003	41.856	4.974	44.922
14.081	36.627	7.595	42.149	4.557	45.798
13.088	37.441	7.232	42.544	4.240	45.875
12.321	38.135	6.893	42.760	3.965	46.278
11.550	38.577	6.562	43.039	3.665	46.992
				3.489	52.122

Table A 2. Experimental weight fraction data for the systems composed of dextran 40 kDa (1) + IL (2) + H_2O (3) at 298.15 K and atmospheric pressure.

$[P_{i(444)1}][Tos]$		**$[P_{444(14)}]Cl$**		**$[P_{4444}]Br$**	
M_W = 388.55		**M_W = 435.15**		**M_W = 339.33**	
100 *w*1	**100 *w*2**	**100 *w*1**	**100 *w*2**	**100 *w*1**	**100 *w*2**
46.395	7.724	47.866	1.701	39.612	10.925
32.328	14.958	39.132	6.177	33.851	13.502
30.774	17.358	20.089	27.620	33.064	14.582
29.451	18.092	18.563	28.698	31.465	16.196
28.301	18.642	17.253	29.102	25.694	21.506
27.346	19.333	15.369	30.547	21.130	23.730
24.777	21.166	13.915	31.456	17.093	27.340
22.551	22.421	12.657	32.317	15.101	28.270
20.091	24.079	11.138	33.755	12.996	30.186
18.617	24.655	9.893	34.680	12.024	30.469
17.000	25.597	8.940	35.116	11.340	30.988
15.736	26.418	8.120	35.837	10.378	32.057
14.552	27.094	7.757	36.211	9.641	32.360
13.642	27.362	7.447	36.330	8.934	33.046
12.786	27.948	7.100	36.449	8.372	33.252
12.134	28.291	6.738	36.939	7.834	33.753
11.437	28.879	6.300	37.222	7.397	34.080
10.766	29.381	5.859	38.040	6.873	34.478
10.212	29.738	5.250	39.693	6.404	34.947
9.711	30.136	4.731	40.925	5.958	35.336
9.219	30.901	2.732	48.249	5.620	35.414
8.888	31.120	1.388	53.768	5.286	35.855
8.392	31.372			5.011	35.994
7.994	31.499			4.773	36.171
7.448	31.924			4.450	36.513
6.923	32.250			4.141	37.120
6.480	32.673			3.871	37.517
6.060	33.173			3.643	37.811
5.724	33.155			2.496	42.305
5.396	33.688			1.994	43.294
5.129	33.781			1.543	43.682
4.929	34.071			0.599	48.235
4.724	33.993				
4.499	34.313				
4.286	34.652				
4.051	34.892				
3.696	35.635				
3.304	36.269				
3.092	40.833				

1.037	49.983

[P_{4441}][$MeSO_4$]		**[P_{4441}][$MeSO_4$]**		**[P_{4441}][$MeSO_4$]**	
***M_W* = 328.45**		***M_W* = 328.45**		***M_W* = 328.45**	
100 *w*1	**100 *w*2**	**100 *w*1**	**100 *w*2**	**100 *w*1**	**100 *w*2**
52.112	8.595	11.915	30.291	8.401	32.626
35.743	14.162	11.618	30.793	8.078	32.755
32.846	18.130	11.582	30.629	7.981	32.915
28.981	20.339	11.306	30.760	7.865	32.918
26.564	21.670	11.031	30.895	7.669	33.054
24.895	22.355	10.754	31.268	7.435	33.189
22.861	23.930	10.754	31.129	7.270	33.525
20.603	25.314	10.510	31.240	7.213	33.251
19.254	25.543	10.242	31.648	7.002	33.473
17.727	26.405	10.043	31.773	6.794	33.630
16.343	27.428	9.793	31.901	6.594	33.720
15.102	28.142	9.415	32.275	6.449	33.842
13.609	29.583	9.381	32.122	6.231	33.949
12.815	29.743	9.120	32.114	2.497	41.691
12.584	29.879	8.879	32.212	0.419	49.597
12.518	29.830	8.704	32.446		
12.194	30.095	8.590	32.549		

Table A 3. Experimental weight fraction data for the systems composed of dextran 100 kDa (1) + IL (2) + H_2O (3) at 298.15 K and atmospheric pressure.

$[P_{i(444)1}][Tos]$		**$[P_{444(14)}]Cl$**		**$[P_{4444}]Br$**	
M_W = 388.55		**M_W = 435.15**		**M_W = 339.33**	
100 *w*1	**100 *w*2**	**100 *w*1**	**100 *w*2**	**100 *w*1**	**100 *w*2**
48.426	3.802	45.365	2.898	41.925	9.131
38.926	9.780	42.135	7.919	35.239	12.322
15.002	27.379	14.200	32.411	26.746	19.799
13.056	28.693	11.710	34.029	20.615	23.427
10.788	30.189	9.748	35.215	17.867	25.201
8.897	31.481	8.555	35.965	16.037	26.636
7.627	32.178	5.968	38.448	14.256	28.656
6.478	32.857	5.353	38.415	12.084	29.322
5.769	33.405	4.207	40.407	10.543	31.222
5.043	34.454	1.991	51.475	9.751	31.196
1.495	42.540	0.802	55.510	9.011	31.896
0.993	48.136			8.397	32.198
				7.816	32.631
				7.356	32.598
				6.870	33.206
				6.273	33.491
				5.653	34.043
				5.149	34.307
				4.599	34.923
				1.004	46.148
				1.004	48.131
$[P_{4441}][MeSO_4]$		**$[P_{4441}][MeSO_4]$**		**$[P_{4441}][MeSO_4]$**	
M_W = 328.45		**M_W = 328.45**		**M_W = 328.45**	
100 *w*1	**100 *w*2**	**100 *w*1**	**100 *w*2**	**100 *w*1**	**100 *w*2**
37.211	12.520	8.267	31.473	3.999	33.453
31.904	15.791	7.727	31.489	3.697	33.685
13.582	28.002	7.133	31.672	3.464	34.015
12.841	28.487	6.552	32.106	3.273	33.857
11.833	28.987	6.032	32.650	3.095	33.990
11.061	29.450	5.603	32.550	34.025	14.959
10.245	30.483	5.175	32.787	1.502	40.595
9.720	30.353	4.707	33.088	3.065	36.011
9.027	31.173	4.241	33.375		

Table A 4. Experimental weight fraction data for the systems composed of maltodextrin DE 16.5-19.5 (1) + IL (2) + H_2O (3) at 298.15 K and atmospheric pressure.

$[P_{i(444)1}][Tos]$		**$[P_{444(14)}]Cl$**		**$[P_{4444}]Br$**	
M_W = 388.55		**M_W = 435.15**		**M_W = 339.33**	
100 *w*1	**100 *w*2**	**100 *w*1**	**100 *w*2**	**100 *w*1**	**100 *w*2**
17.810	44.288	24.160	36.344	24.240	34.985
16.526	45.555	20.509	37.701	20.429	36.677
14.995	46.283	18.891	38.292	17.553	39.018
13.147	47.541	17.054	39.272	14.531	41.211
11.577	48.268	15.481	40.031	12.480	42.787
10.997	48.960	14.189	40.764	10.869	44.017
10.018	49.681	13.308	41.205	9.584	44.927
9.111	50.388	11.780	42.406	8.655	45.705
8.444	50.974	10.765	42.742		
7.476	51.843	9.820	43.741		
6.376	53.411	8.983	44.126		
4.754	55.619	7.307	45.234		
		6.201	46.625		
		5.048	48.028		
		4.269	49.244		
$[P_{4441}][MeSO_4]$		**$[P_{4441}][MeSO_4]$**		**$[P_{4441}][MeSO_4]$**	
M_W = 328.45		**M_W = 328.45**		**M_W = 328.45**	
100 *w*1	**100 *w*2**	**100 *w*1**	**100 *w*2**	**100 *w*1**	**100 *w*2**
26.265	35.332	11.823	41.737	7.157	44.344
22.826	36.911	10.967	42.064	6.789	44.489
17.349	38.972	10.219	42.662	6.265	44.807
15.711	39.704	9.430	43.354	5.708	45.891
14.268	40.777	8.760	43.503	5.207	46.008
12.954	41.250	8.118	44.076		

Table A 5. Experimental weight fraction data for the systems composed of maltodextrin DE 13.0-17.0 (1) + IL (2) + H_2O (3) at 298.15 K and atmospheric pressure.

$[P_{i(444)1}][Tos]$		**$[P_{444(14)}]Cl$**		**$[P_{4444}]Br$**	
M_W = 388.55		**M_W = 435.15**		**M_W = 339.33**	
100 *w*1	**100 *w*2**	**100 *w*1**	**100 *w*2**	**100 *w*1**	**100 *w*2**
20.844	42.403	24.812	34.131	24.807	34.227
19.558	42.931	22.338	36.026	20.681	35.816
18.401	43.379	20.763	36.707	17.473	38.587
16.928	44.370	19.061	37.703	14.235	41.408
15.407	45.341	17.128	38.660	12.052	42.692
14.395	46.061	15.862	39.545	10.599	43.695
13.323	46.534	13.920	41.004	9.322	44.832
12.071	47.221	12.297	42.077	8.393	45.503
10.738	48.378	11.109	42.493	7.633	46.125
8.233	49.504	9.843	43.696	6.747	46.563
6.442	51.521	8.888	44.044	5.947	47.605
5.424	52.850	7.959	44.581	5.295	48.821
		6.913	45.922		
		5.715	47.702		
		4.807	48.850		
$[P_{4441}][MeSO_4]$		**$[P_{4441}][MeSO_4]$**		**$[P_{4441}][MeSO_4]$**	
M_W = 328.45		**M_W = 328.45**		**M_W = 328.45**	
100 *w*1	**100 *w*1**	**100 *w*1**	**100 *w*2**	**100 *w*1**	**100 *w*2**
25.215	36.852	10.356	42.398	6.236	44.314
21.269	37.516	9.516	42.834	5.457	45.130
14.145	40.378	7.300	43.798	5.249	45.204
12.582	41.215	6.900	44.012	4.958	45.370
11.314	41.850	6.605	44.176		

Table A 6. Experimental weight fraction data for the systems composed of maltodextrin DE 16.5-19.5 (1) + IL (2) + H_2O (3) at 298.15 K and atmospheric pressure.

[C_4mim][CF_3SO_3]		**[C_2mim][CF_3SO_3]**		**[C_4mim][BF_4]**	
***M_W* = 288.29**		***M_W* = 260.24**		***M_W* = 226.02**	
100 *w*1	**100 *w*2**	**100 *w*1**	**100 *w*2**	**100 *w*1**	**100 *w*2**
27.257	18.768	29.359	29.594	18.220	18.400
24.245	20.990	26.798	30.616	17.580	19.415
21.184	23.871	24.418	31.973	16.785	20.245
19.305	25.023	23.397	32.409	15.869	20.331
17.042	27.692	21.638	33.450	15.206	21.037
15.579	29.432	20.225	34.309	13.372	23.101
14.516	30.226	18.898	34.931	13.052	23.684
13.592	31.145	17.586	35.568	12.392	24.573
12.698	31.467			11.096	28.429
11.684	32.381			10.227	32.037
10.783	32.643				
10.059	33.200				
9.502	33.638				
8.763	34.172				
8.264	34.463				
[C_4mim][$EtSO_4$]		**[C_4mim][SCN]**		**[C_4mim][SCN]**	
***M_W* = 264.33**		***M_W* = 197.3**		***M_W* = 197.3**	
100 *w*1	**100 *w*2**	**100 *w*1**	**100 *w*2**	**100 *w*1**	**100 *w*2**
31.112	22.334	20.777	48.405	12.150	50.742
26.780	23.786	18.770	48.836	11.153	51.372
19.718	37.185	16.163	49.344	10.124	51.937
14.673	40.260	15.086	49.515	8.487	52.524
10.114	46.499	14.016	50.286	7.832	53.239
		12.976	50.485	7.217	53.343

Table A 7. Experimental weight fraction data for the systems composed of maltodextrin DE 13.0-17.0 (1) + IL (2) + H_2O (3) at 298.15 K and atmospheric pressure.

[C_4mim][CF_3SO_3]		**[C_2mim][CF_3SO_3]**		**[C_4mim][BF_4]**	
***M_W* = 288.29**		***M_W* = 260.24**		***M_W* = 226.02**	
100 *w*1	**100 *w*2**	**100 *w*1**	**100 *w*2**	**100 *w*1**	**100 *w*2**
32.892	16.810	28.015	29.775	37.922	9.278
28.202	19.418	26.858	30.386	35.608	10.125
25.075	21.700	25.650	31.067	33.374	10.932
22.444	22.354	24.715	31.742	25.926	12.753
19.857	24.486	23.453	32.874	23.636	13.673
17.846	26.590	21.581	33.337	21.712	15.235
16.110	28.519	20.571	33.831	20.589	16.023
14.690	29.670	19.720	33.830	19.175	16.511
13.483	30.845	19.313	34.091	18.626	16.922
12.502	31.057	18.424	35.012	17.951	17.890
11.557	31.732	14.434	38.604	17.269	18.749
10.777	32.274	14.040	38.694	16.609	18.929
10.115	32.624	13.217	38.840	16.240	19.196
9.337	33.034	12.713	38.846	15.454	19.919
8.904	33.193	11.041	40.040	14.565	21.110
8.330	33.559	10.292	40.727	13.766	22.309
7.806	34.115	9.337	40.510	13.048	23.336
7.284	34.536	8.374	40.430	12.413	24.339
6.660	34.774	7.492	41.365	11.618	26.574
6.027	35.241			10.715	29.777
5.560	35.780			0.393	69.362
5.118	36.231				
4.708	36.421				
[C_4mim][$EtSO_4$]		**[C_4mim][SCN]**			
***M_W* = 264.33**		***M_W* = 197.3**			
100 *w*1	**100 *w*2**	**100 *w*1**	**100 *w*2**		
17.941	37.725	18.869	48.249		
11.648	45.961	17.037	49.374		
6.197	52.794	13.976	49.947		
14.789	43.246	12.859	50.616		
9.775	48.296	11.668	51.249		
9.167	49.137	9.951	52.294		
8.220	49.379	8.494	53.044		
		7.581	53.229		

Appendix B

Calibration Curves

Figures B1 to B3 depict the calibration curves (absorbance *vs.* concentration) for L-tyrosine, L-tryptophan and L-phenylalanine.

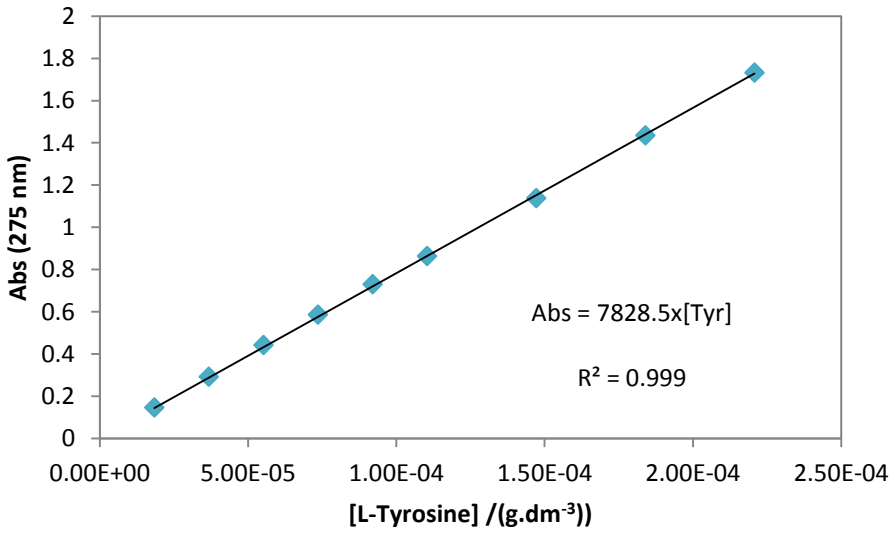

Figure B 1. Calibration curve for L-tyrosine at 275 nm.

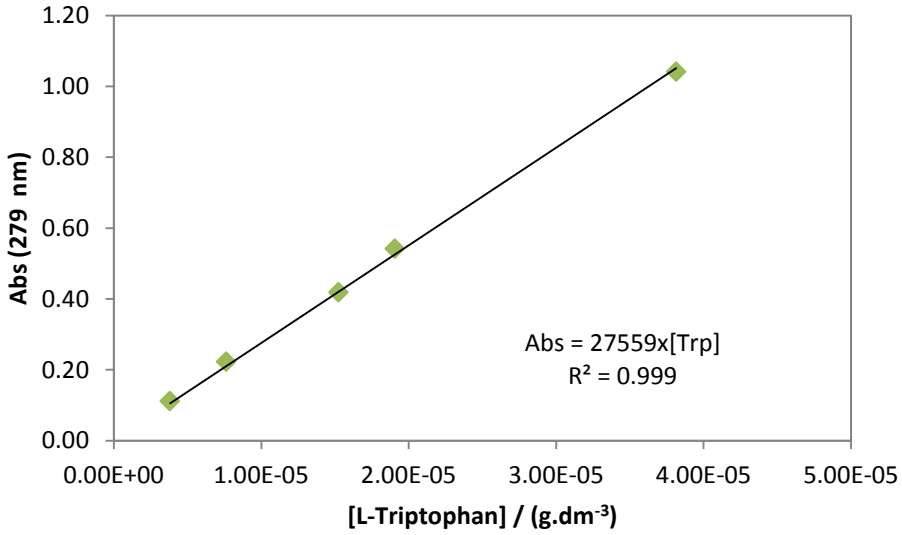

Figure B 2. Calibration curve for L-tryptophan at 279 nm.

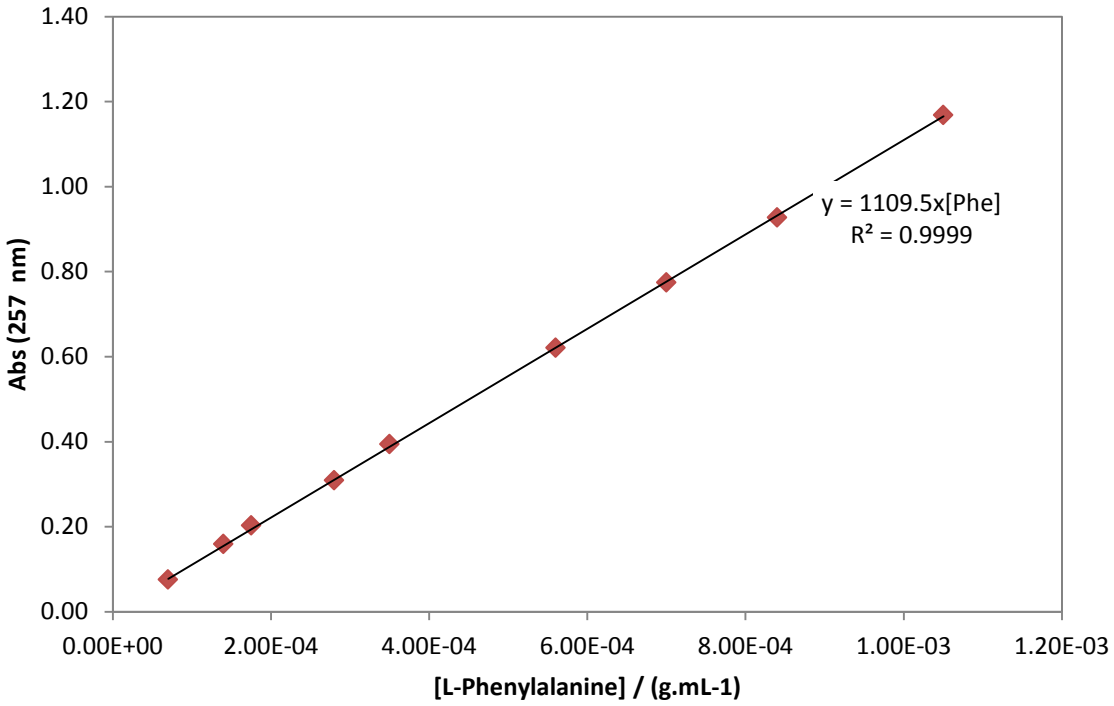

Figure B 3. Calibration curve for L-phenylalanine at 257 nm.